Advanced 21-cm Cosmology Workshop @ NISER

NCRA • TIFR

Probing the Epoch of Reionization with CMB Anisotropies

Divesh Jain

NCRA-TIFR

Fig Credit: https://kipac.stanford.edu/research/projects/cmb-stage-4

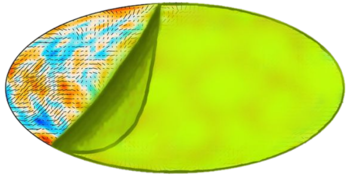

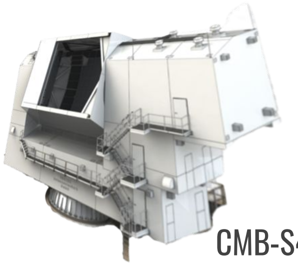

CMB-S4

In collaboration with
Tirthankar Roy Choudhury (NCRA-TIFR Pune)
Suvodip Mukherjee (TIFR Mumbai)
Srinivasan Raghunathan (University of Illinois)
Sourabh Paul (McGill University)

21-cm Cosmology

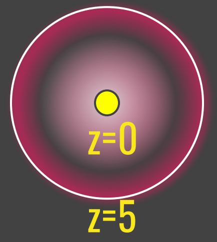

21-cm Cosmology

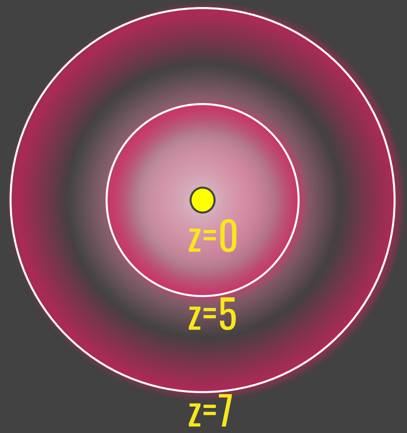

21-cm Cosmology

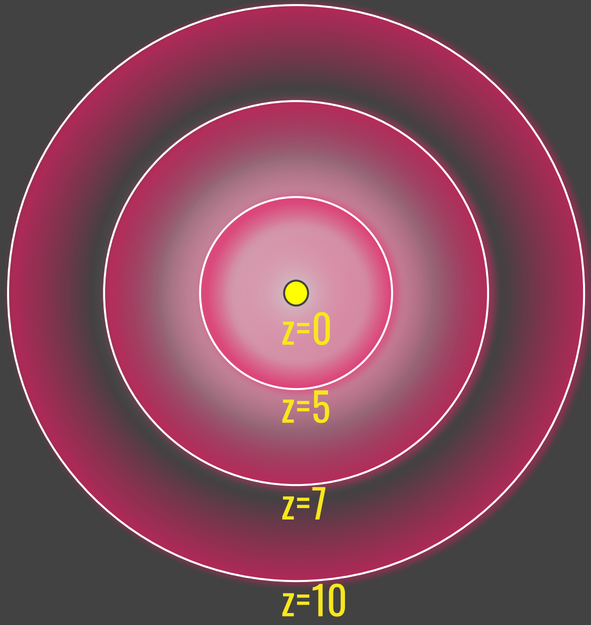

21-cm Cosmology

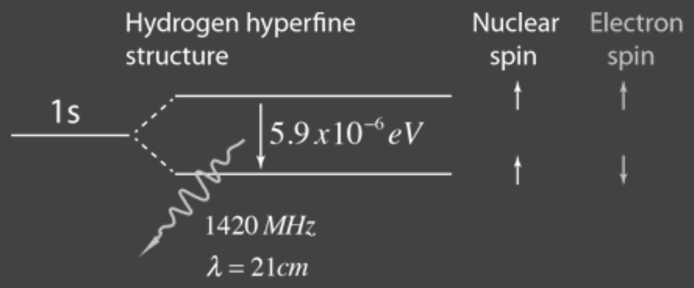

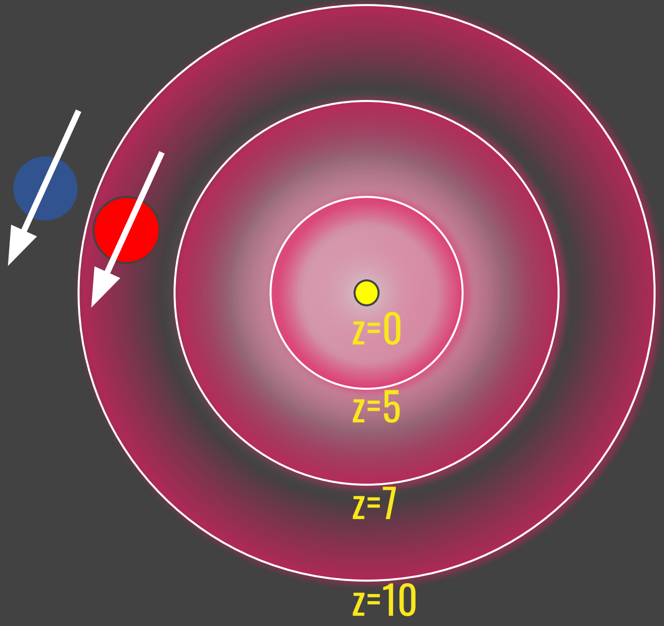

21-cm Cosmology

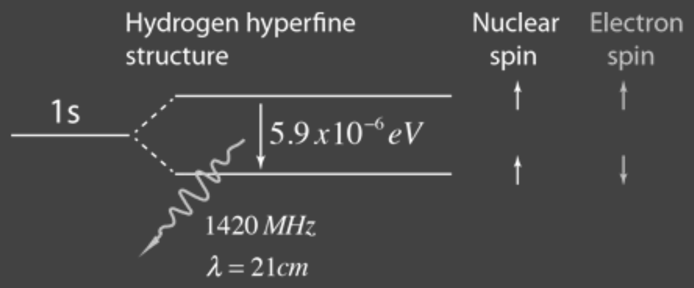

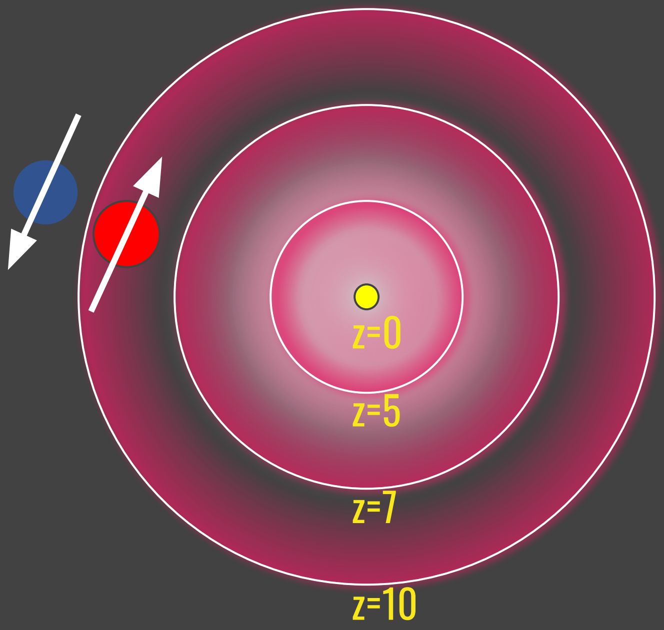

21-cm Cosmology

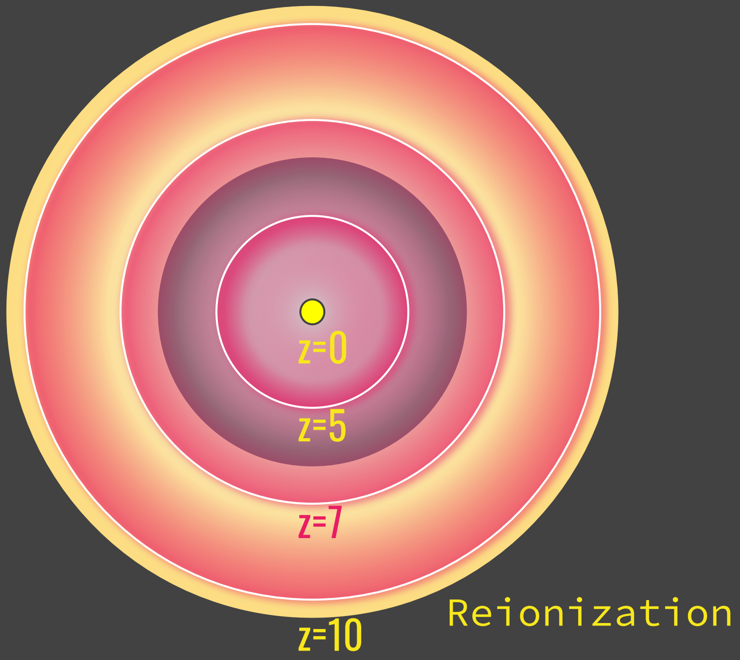

Reionization

Review articles:
T.R. Choudhury arXiv:2209.08558
Gnedin & Madau arXiv:2208.02260

Reionization is a process whereby hydrogen and helium in the Intergalactic Medium is ionized by the radiation from first luminous sources.

Why you should be excited?

- When did the first luminous sources form in the Universe?
- Was reionization driven by rare massive halos or was it driven by lighter halos?
- Was reionization a fast process or a slow process?
- How inhomogeneous was the process of reionization?

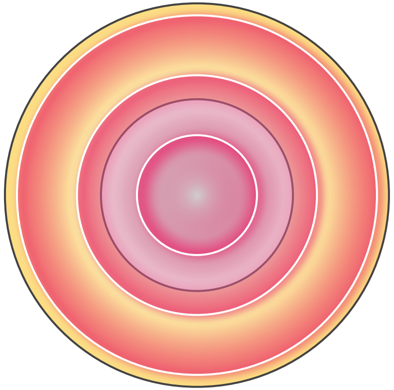

Reionization

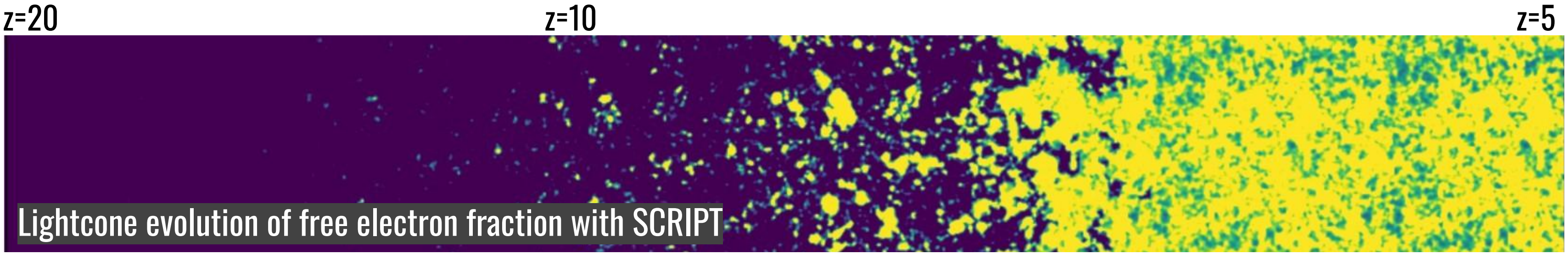

Lightcone evolution of free electron fraction with SCRIPT

Just before the dark

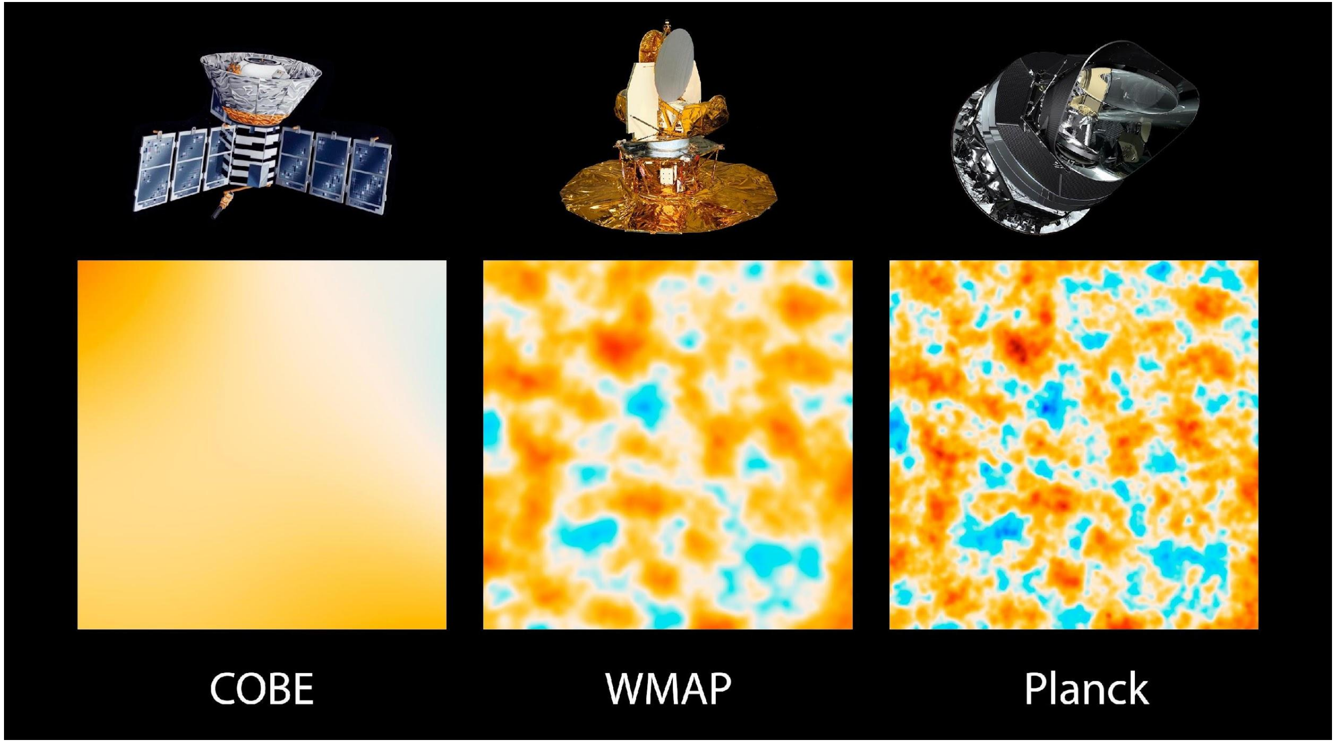

The night was "not" darkest just before the dawn

The CMB anisotropies: Holy Grail of Cosmology

All-sky maps

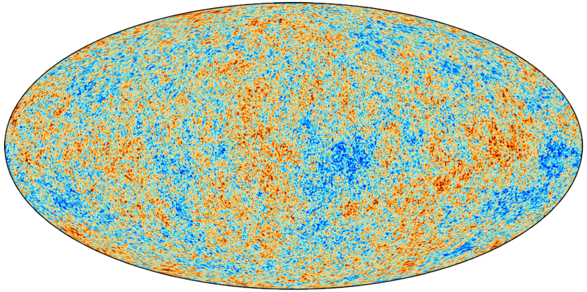

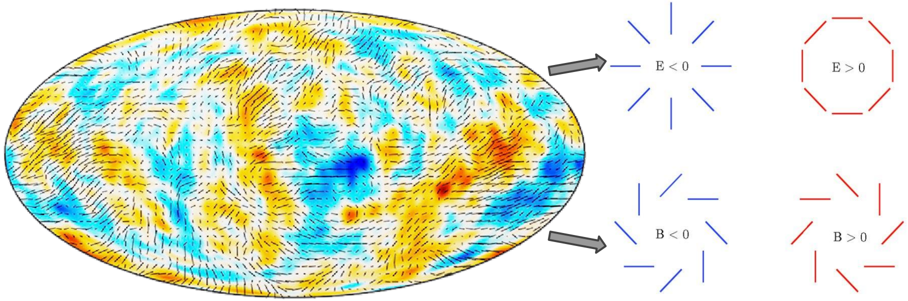

Planck 2018

Temperature Anisotropies

Polarization Anisotropies

Power spectrum

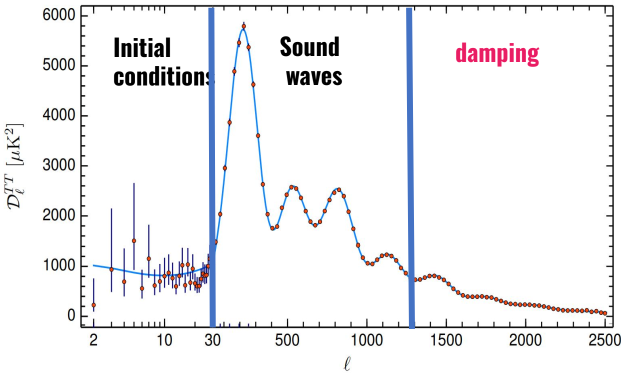

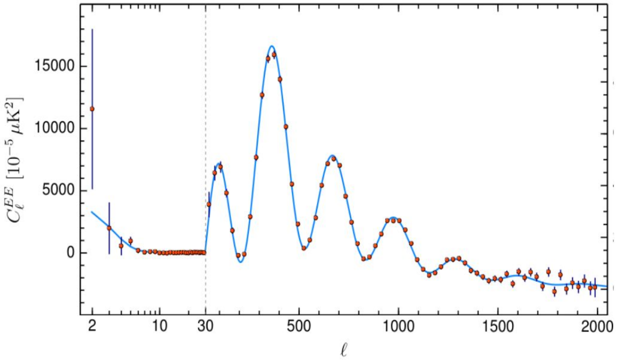

Reionization imprints on CMB

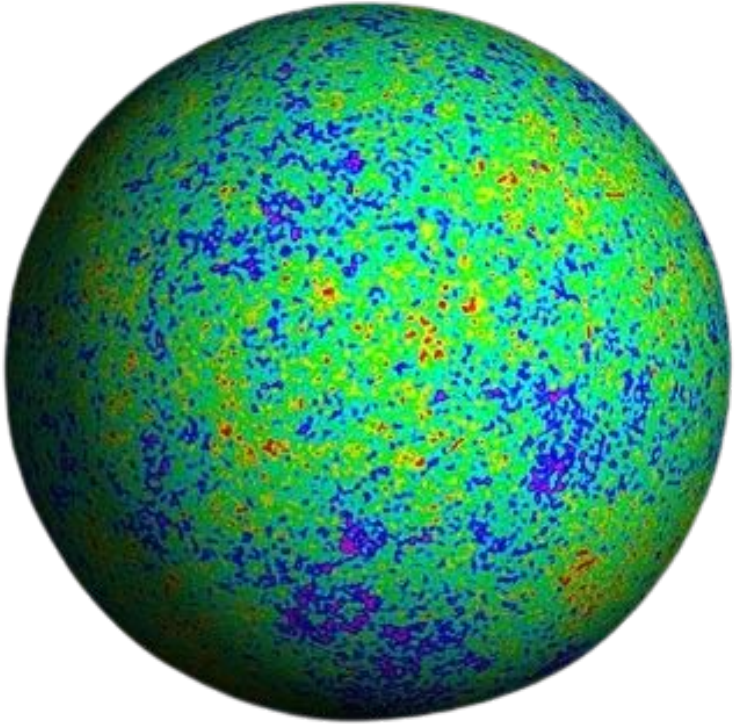

Fig Credit: Max Tegmark

Reionization imprints on CMB

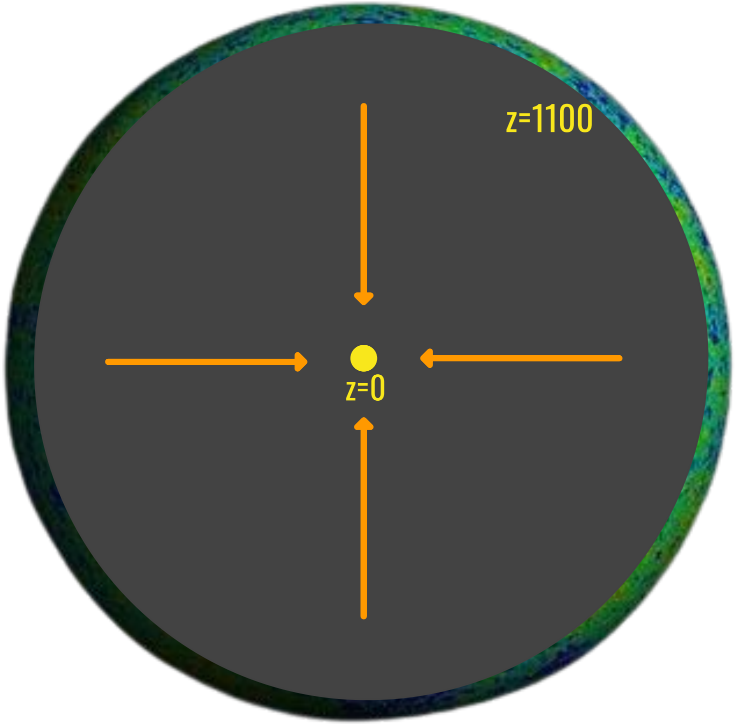

Reionization imprints on CMB

- CMB photons re-scatters off free electrons in the era of Reionization.
- Thomson scattering of CMB photons modify the temperature and polarization anisotropies of CMB

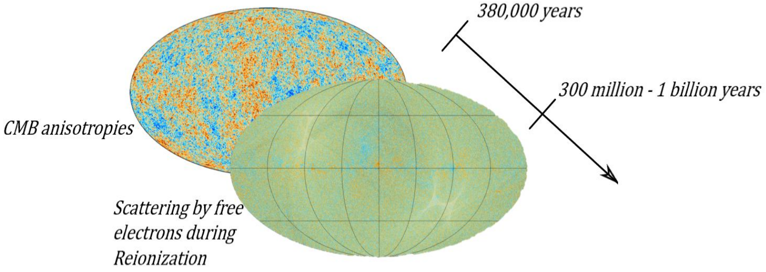

Rescattering of CMB during Reionization era

Reionization imprints on CMB

- CMB photons re-scatters off free electrons in the era of Reionization.
- Thomson scattering of CMB photons modify the temperature and polarization anisotropies of CMB

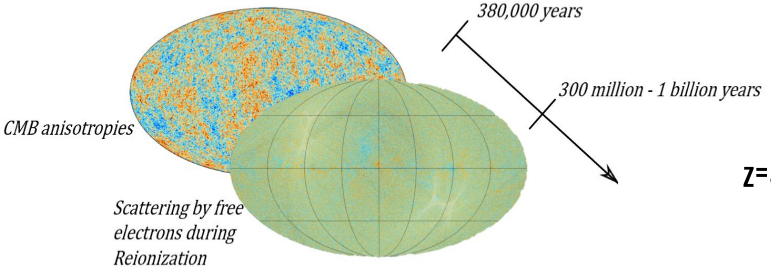

Rescattering of CMB during Reionization era

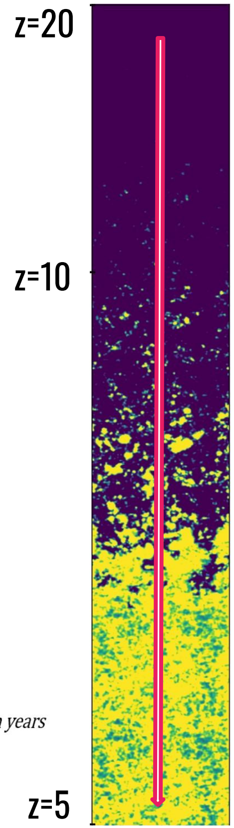

Reionization imprints on CMB

- CMB photons re-scatters off free electrons in the era of Reionization.
- Thomson scattering of CMB photons modify the temperature and polarization anisotropies of CMB

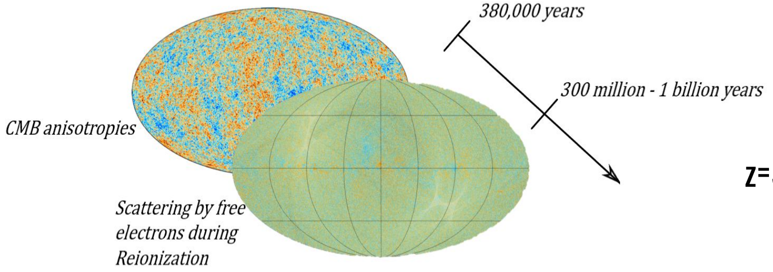

Rescattering of CMB during Reionization era

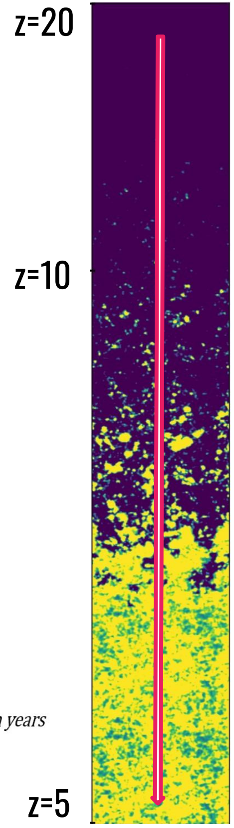

Reichardt et al. 2015

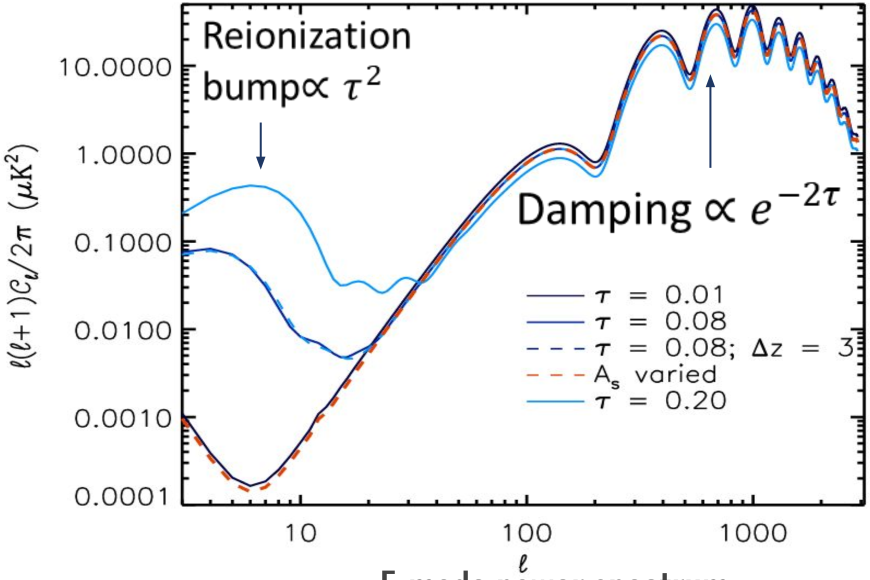

E-mode power spectrum

$$\tau^{\rm obs} = 0.054 \pm 0.007$$

Planck 2018

Probe of :

- Reionization timing and duration

Reionization imprints on CMB

- CMB photons re-scatters off free electrons in the era of Reionization.
- Thomson scattering of CMB photons modify the temperature and polarization anisotropies of CMB

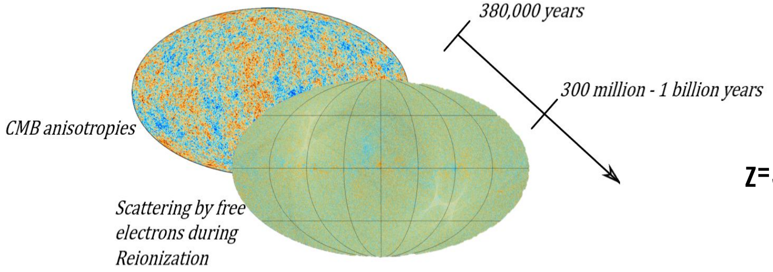

Rescattering of CMB during Reionization era

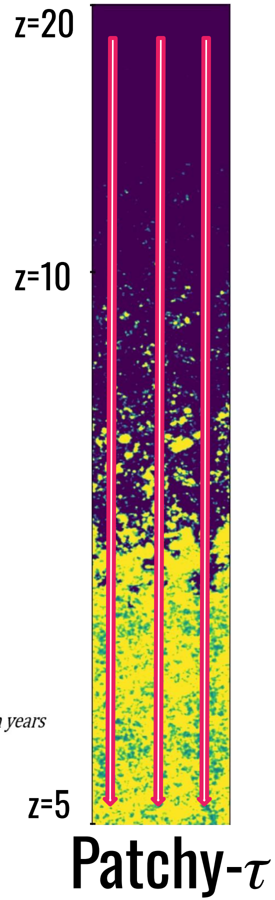

Reionization imprints on CMB

- The patchy E & B - mode polarization arises as a result of Thomson scattering of CMB temperature quadrupole off the inhomogeneous ionized field.
- The strength of the power spectrum of fluctuations in free electron fraction x_e.

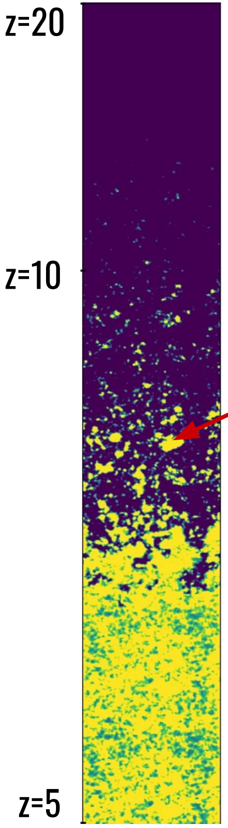

Patchy-τ

$$\tau(\hat{n}) = \bar{\tau} + \Delta\tau(\hat{n})$$

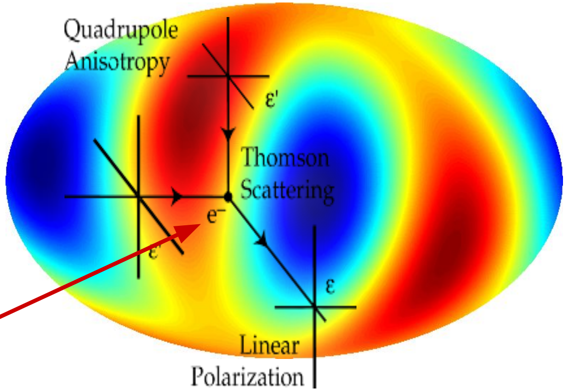

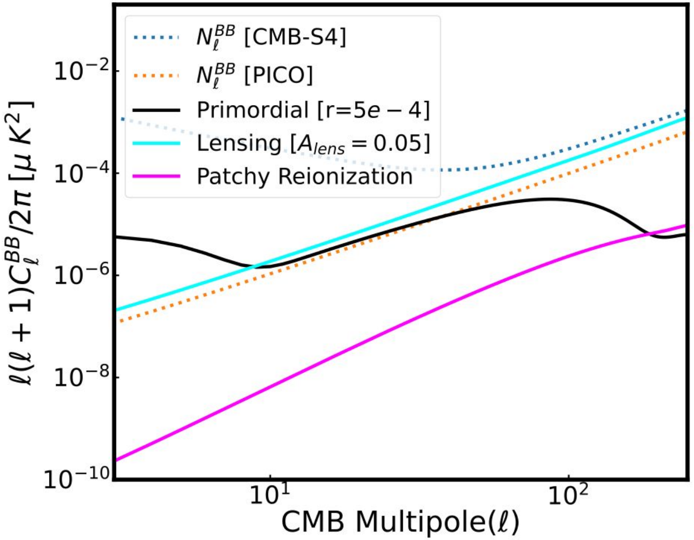

Patchy-Scattering Polarization

Reionization imprints on CMB

- kinematic-Sunyaev-Zeldovich effect: Doppler shift in CMB photons as they scatter off ionized bubbles with non-zero bulk velocity

$$\frac{\Delta T(\hat{n})}{T_0} = -\int_0^{\tau} d\tau\; e^{-\tau(\chi)}\, \frac{\hat{n}\cdot\mathbf{v}}{c}$$

- Total kSZ power:

  Patchy kSZ + Homogeneous kSZ

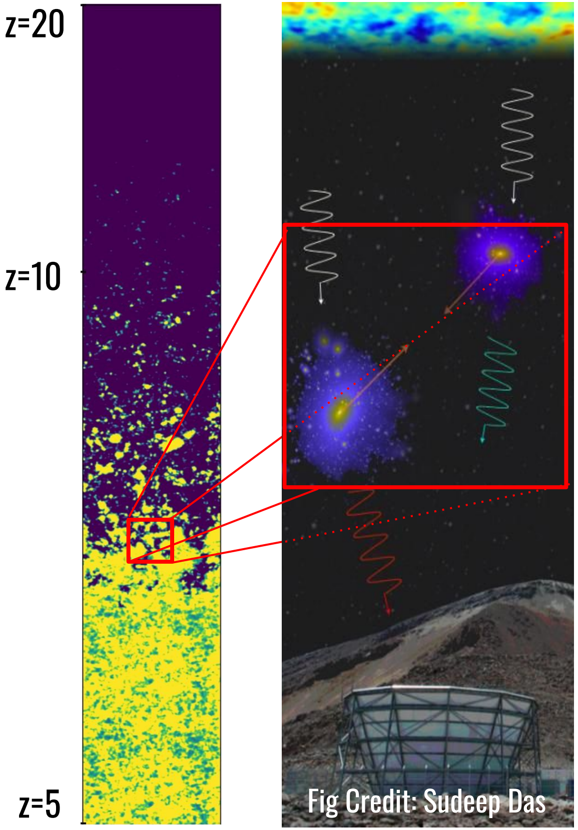

Patchy-τ **Patchy-kSZ**

$$\tau(\hat{n}) = \bar{\tau} + \Delta\tau(\hat{n})$$

Planck 2015

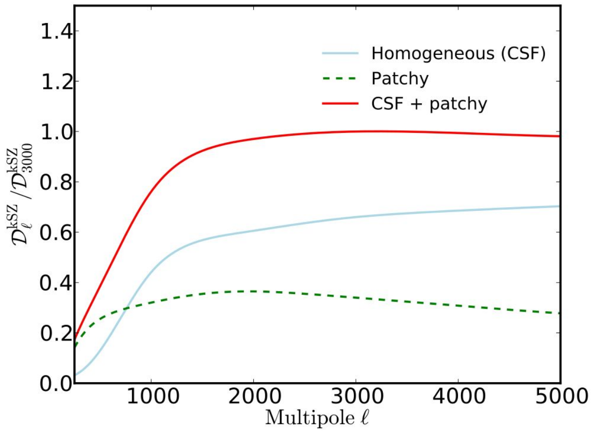

First 3σ measurement =

$D^{\rm kSZ,obs}_{\ell=3000} = 3.0 \pm 1.0\mu K^2$

(SPT 2021)

Probe of :

- Reionization History
- Morphology of Ionized regions
- Large-scale velocity field

CMB missions:

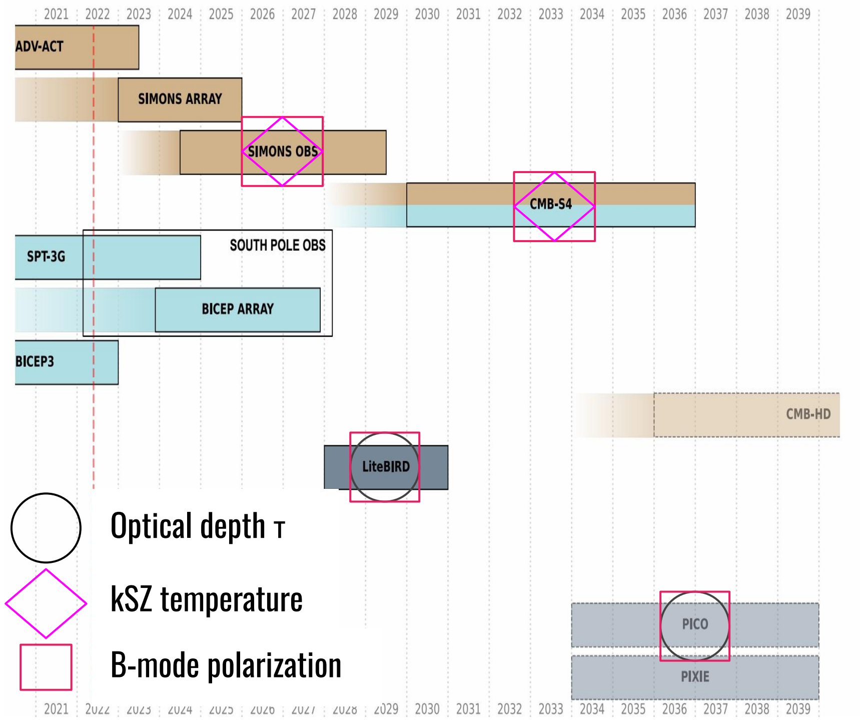

Simons Observatory

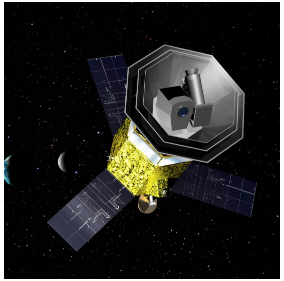

LiteBIRD

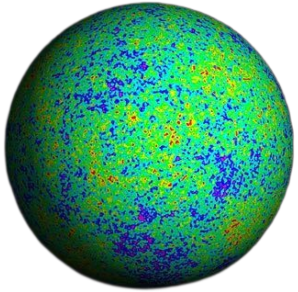

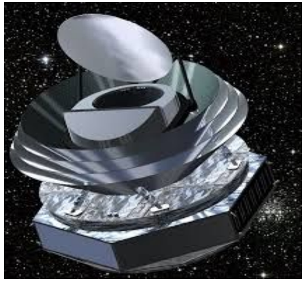

PICO

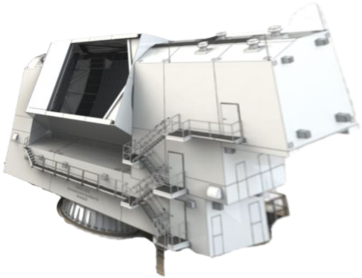

CMB-S4

Connecting CMB observables to Reionization physics

CMB Observables Parameter Space

CMB Observables $\tau,\ D_\ell^{\rm kSZ},\ D_\ell^{\rm BB}$

Current Constraints:

$\tau^{\rm obs} = 0.054 \pm 0.007$ Planck 2018

$D_{\ell=3000}^{\rm kSZ,obs} = 3.0 \pm 1.0 \mu K^2$ SPT 2021

Future Constraints:

$$\tau,\ D_\ell^{\rm kSZ},\ D_\ell^{\rm BB}$$

Open Questions from Reionization

- When did the first luminous sources form in the Universe?
- Was reionization driven by rare massive halos or was it driven by lighter halos?
- Was reionization a fast process or a slow process?
- How inhomogeneous was the process of reionization?

Reionization simulations with SCRIPT:

SCRIPT is a photon-conserving semi-numerical reionization scheme (Choudhury & Paranjape 2018)

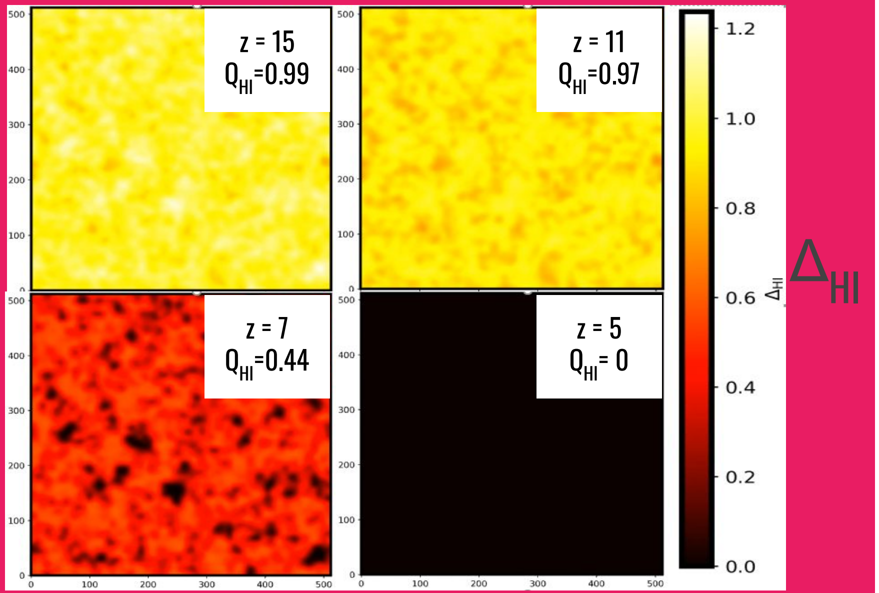

SCRIPT: https://bitbucket.org/rctirthankar/script/src/master/

Advantages of SCRIPT:

- Fast parameterization of reionization sources
- Resolution-independent large-scale ionization maps
- Generate maps of interest (e.g. 21 cm, kSZ, τ maps)
- Vital for parameter estimation due to semi-numerical nature.

SCRIPT Bootcamp:

- Input : Dark matter snapshots at redshift z
- Output : Ionization fraction $x_{HII}(\mathbf{x},z)$
- Source Parameterization : $log\ M_{min}, \zeta$
- Parameters of interest for CMB modelling:
  - $x_e(\mathbf{x},z)=\chi_{He} x_{HII}(\mathbf{x},z)$
  - $Q_{HII}(z)=\langle x_{HII}(\mathbf{x},z)(1+\delta)\rangle$
  - $\Delta_e=x_e(1+\delta)$
  - $q=\Delta_e(\mathbf{v}/c)$
- Evaluation of ionization maps across reionization redshifts : CMB observables of Reionization

Framework for self-consistent evaluation of CMB anisotropies

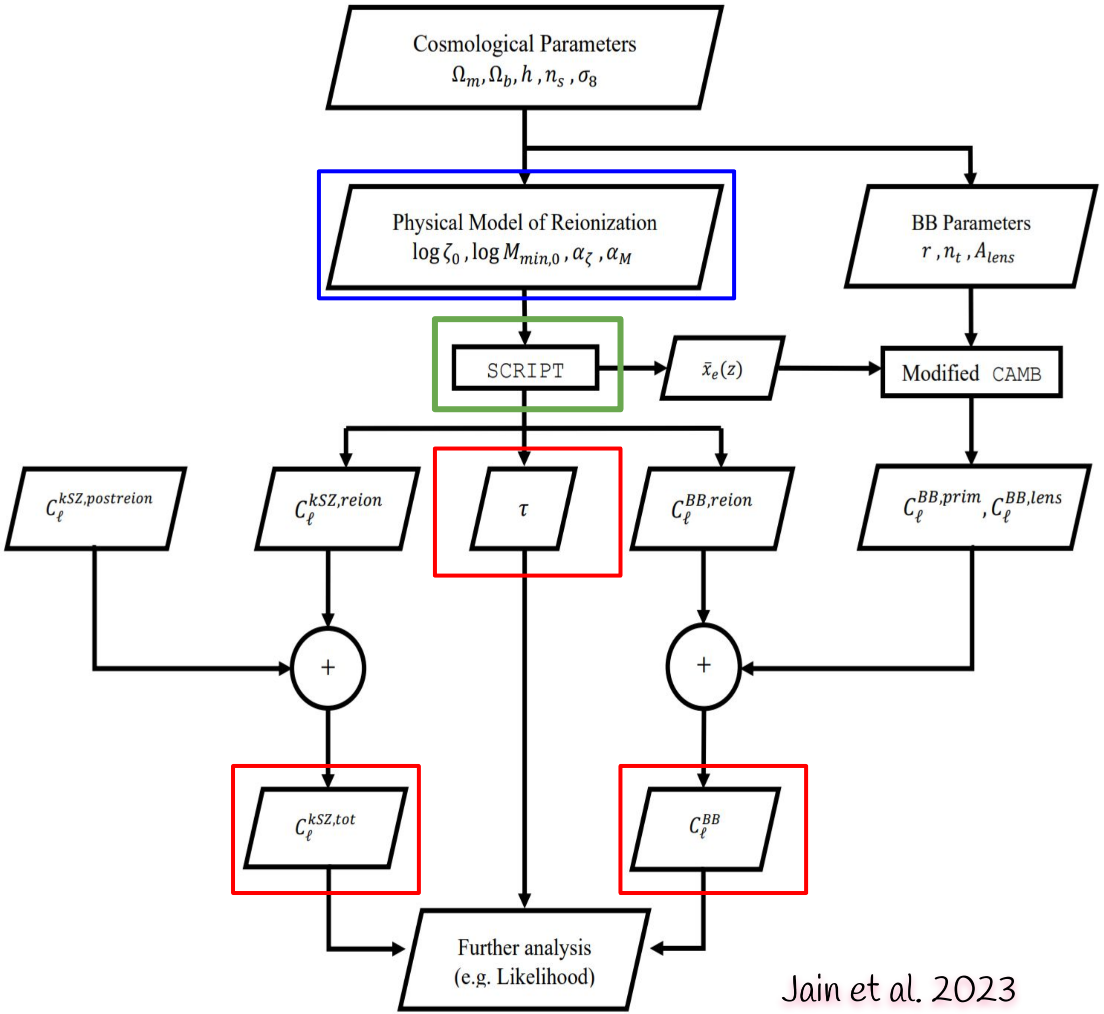

Jain et al. 2023

Framework for self-consistent evaluation of CMB anisotropies

- Minimum mass of haloes that host ionizing source

$$M_{\text{min}}(z) = M_{\text{min},0}\left(\frac{1+z}{9}\right)^{\alpha_M}$$

- Ionizing efficiency of the sources

$$\zeta(z) = \zeta_0\left(\frac{1+z}{9}\right)^{\alpha_\zeta}$$

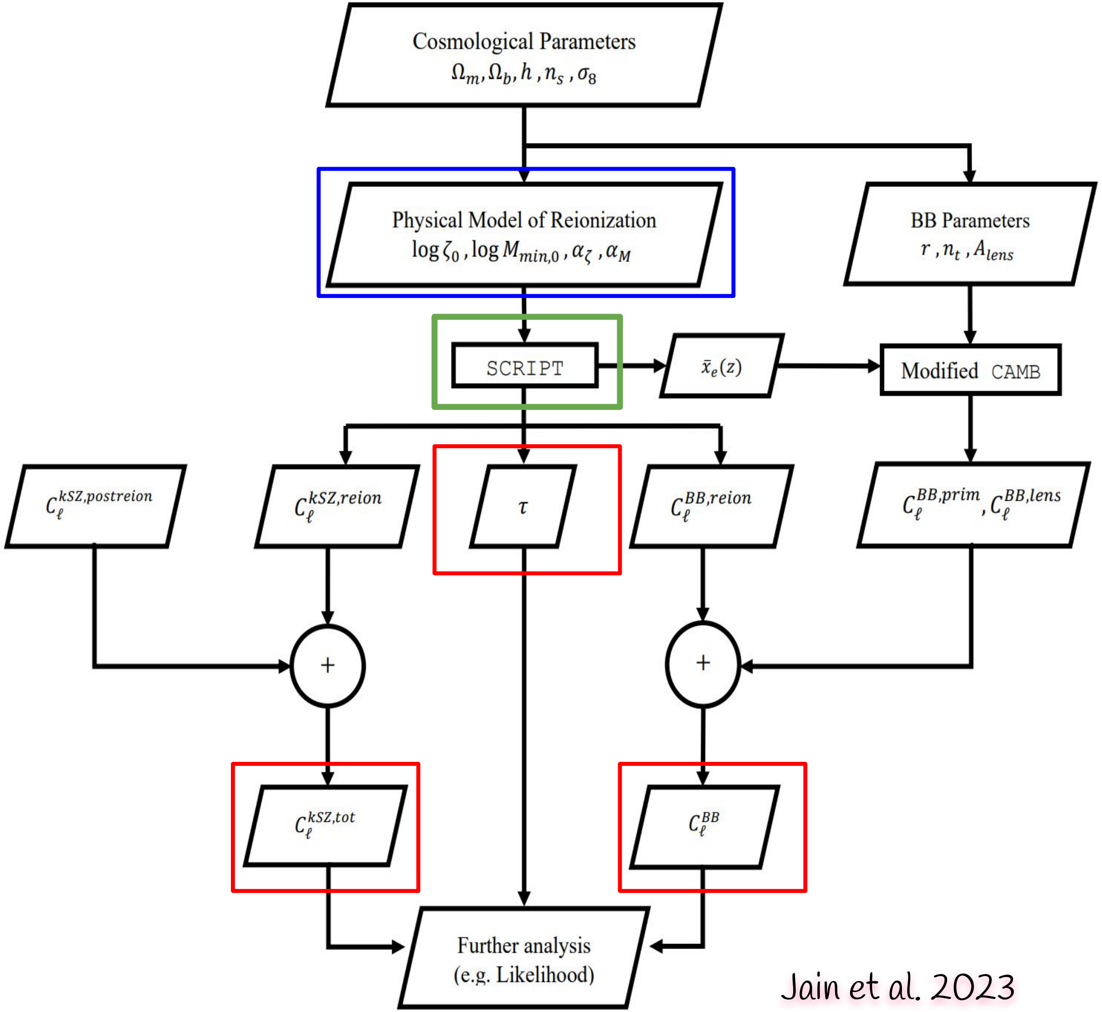

Jain et al. 2023

Constraints on reionization model parameters with available CMB data

Current Constraints:

$$D_{\ell=3000}^{\mathrm{kSZ,obs}} = 3.0 \pm 1.0 \mu K^2$$

$$\tau^{\mathrm{obs}} = 0.054 \pm 0.007$$

The important takeaways are:

- The Planck + SPT data prefers $\log_{10}(M_{min}) > 9$ indicative of suppressed star formation in low mass haloes as a result of radiative feedback at $z \sim 8$.
- Data prefers negative α_ζ indicative of more efficient cooling and star formation or increased escape fraction at lower redshifts.
- Width of reionization : $\Delta z = 1.19^{+0.27}_{-0.53}$

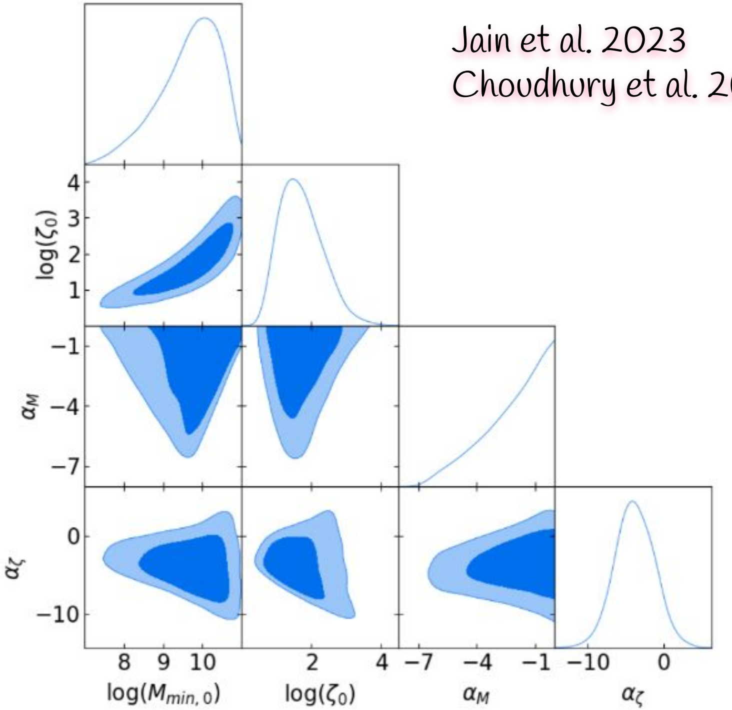

Jain et al. 2023
Choudhury et al. 2022

Planck (τ) + SPT (kSZ)	
Parameter	*68% limits*
$log(M_{min,0})$	$\mathbf{9.69^{+1.02}_{-0.49}}$
$log(\zeta_0)$	$1.70^{+0.49}_{-0.76}$
α_M	> 2.78
α_ζ	$\mathbf{-3.81^{+2.58}_{-2.52}}$

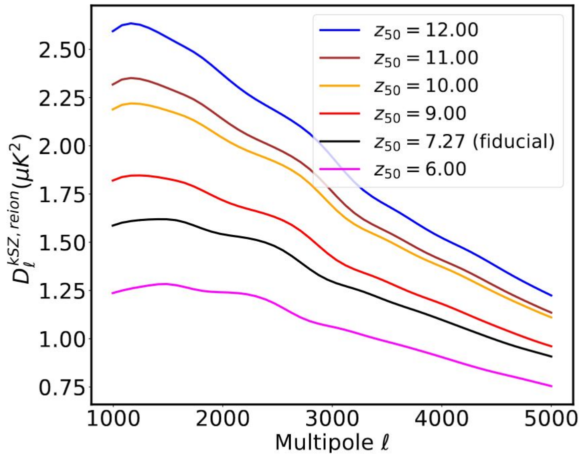

Variation in patchy kSZ with midpoint of reionization, z_{mid}.

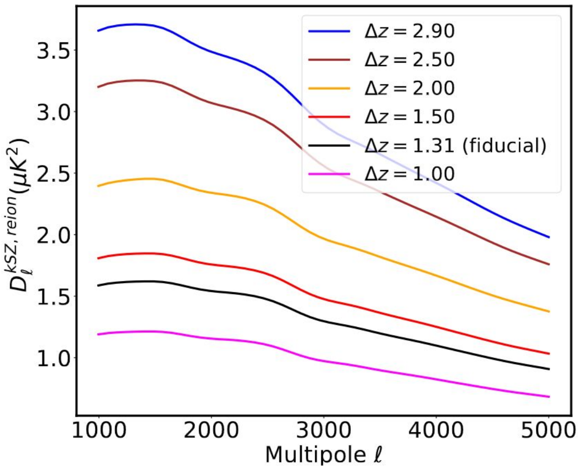

Variation in patchy kSZ with midpoint of reionization, Δz.

Beyond $\ell = 3000$!

kSZ power spectrum:

- Amplitude [Duration of reionization, Mid-point of reionization]
- Shape

Zahn el. 2012
Battaglia et al. 2013

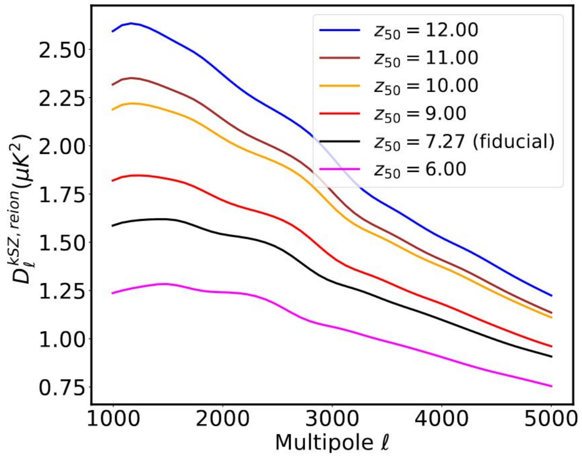

Variation in patchy kSZ with midpoint of reionization, $z_{\rm mid}$.

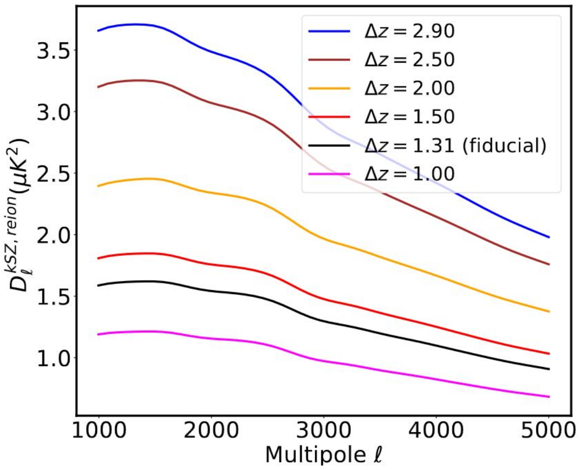

Variation in patchy kSZ with midpoint of reionization, Δz.

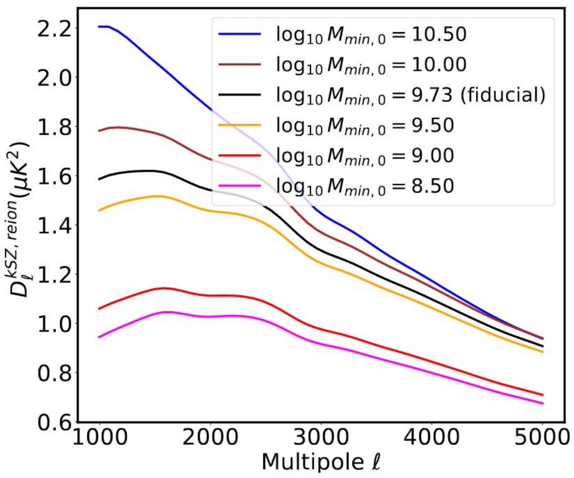

Variation in patchy kSZ with minimum mass of halo at $z=8$, $\log_{10} \mathrm{M}_{\mathrm{min},0}$.

Beyond $\ell = 3000$!

Gorce et al. 2020
Paul et al. 2021
This work!

kSZ power spectrum:

- Amplitude [Duration of reionization, Mid-point of reionization, inhomogeneity in IGM]
- Shape [size of the ionized regions "bubbles"]

Jain et al. (submitted)
arXiv:2311.00315

Resolving Foreground in kSZ extraction

- kSZ is difficult to measure because of the presence of foregrounds.
- The dominant foregrounds being Thermal Sunyaev Zeldovich (tSZ) effect and Dusty Star Forming Galaxy (DSFG) which makes up the Cosmic Infrared Background (CIB).
- The standard approach has been to measure the kSZ power spectrum using simulation-based templates.
- If these templates are misestimated, this method can bias the kSZ estimation.

Reichardt et al. 2021 - *First detection of kSZ*

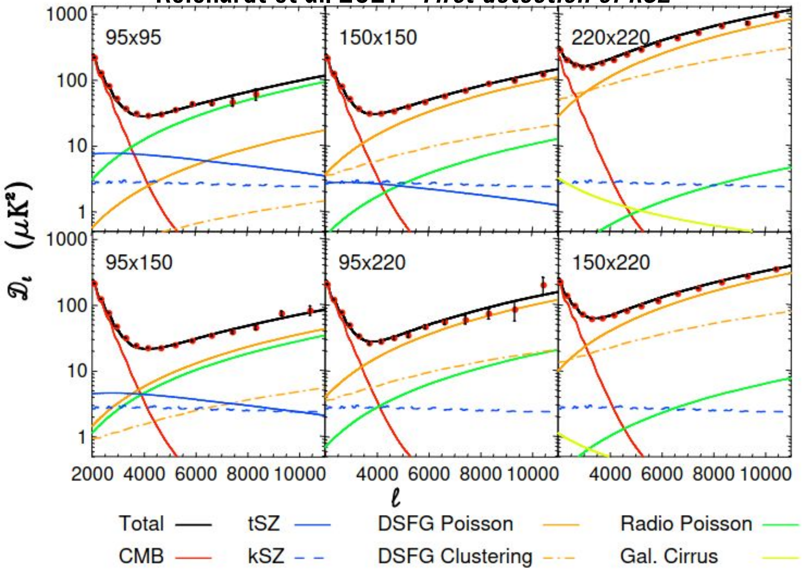

In the above Figure,

- Red markers denote the power spectra measured with the 95, 150, and 220 GHz SPT data.
- The black line denote the best fit model describing the data
- The coloured curves represent the power in each component of the model.

The Cross-ILC kSZ extraction

- The Internal Linear Combination (ILC) technique uses frequency dependence of the signals to form a weighted linear combination of frequency maps.
- The total variance from experimental noise and foreground is minimized.
- The Cross-ILC involves constructing two CMB maps where each map is designed to null the response of different foreground signals (tSZ and CIB). (Raghunathan & Omori 2023)
- Then use the cross-power spectrum for the two maps to recover the kSZ power spectrum estimation accurately.

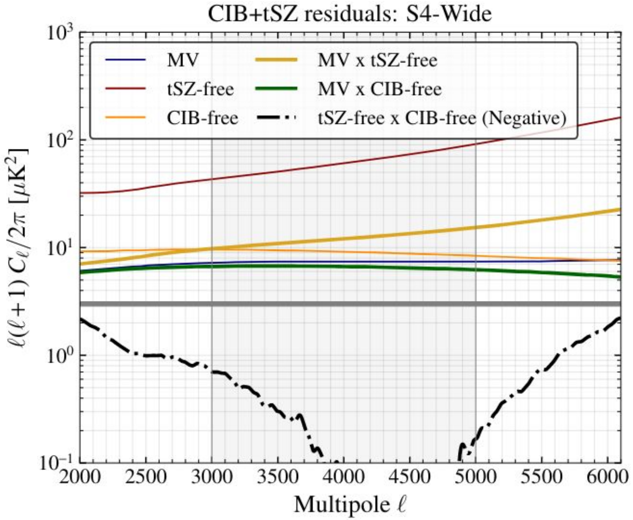

The CIB+tSZ residual shown in black dash dotted curve is almost an order of magnitude lower than kSZ (grey line at 3μK^2) for $\ell \in$ [3500, 5000].

Raghunathan & Omori 2023

In the above figure,

- Grey line refers to an assumed amplitude of kSZ at $D_{\ell=3000}^{\rm kSZ} = 3.0\mu K^2$
- Dark blue line represents represents Minimum Variance extraction

The Cross-ILC kSZ extraction

- The Internal Linear Combination (ILC) technique uses frequency dependence of the signals to form a weighted linear combination of frequency maps.
- The total variance from experimental noise and foreground is minimized.
- The Cross-ILC involves constructing two CMB maps where each map is designed to null the response of different foreground signals (tSZ and CIB). (Raghunathan & Omori 2023)
- Then use the cross-power spectrum for the two maps to recover the kSZ power spectrum estimation accurately.

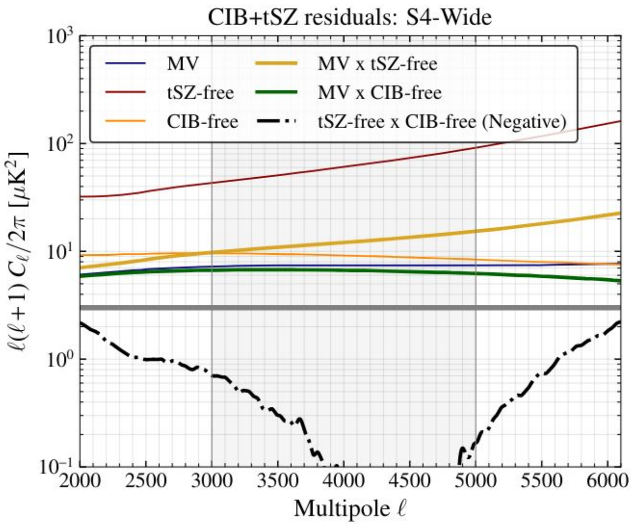

The CIB+tSZ residual shown in black dash dotted curve is almost an order of magnitude lower than kSZ (grey line at $3\mu K^2$) for $\ell \in [3500, 5000]$.

Raghunathan & Omori 2023

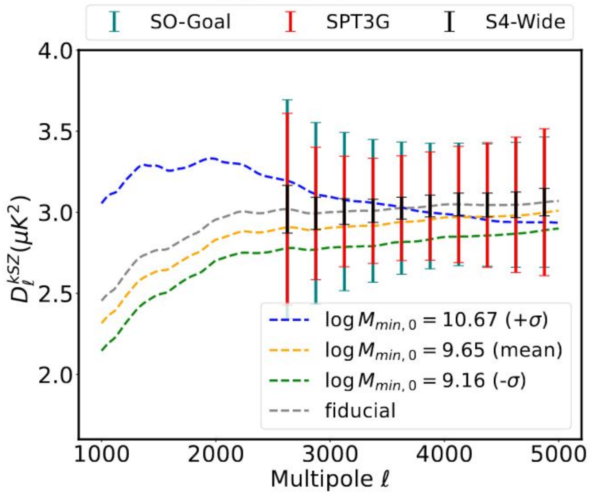

kSZ power with Cross-ILC error bars

Reionization forecast for upcoming experiments

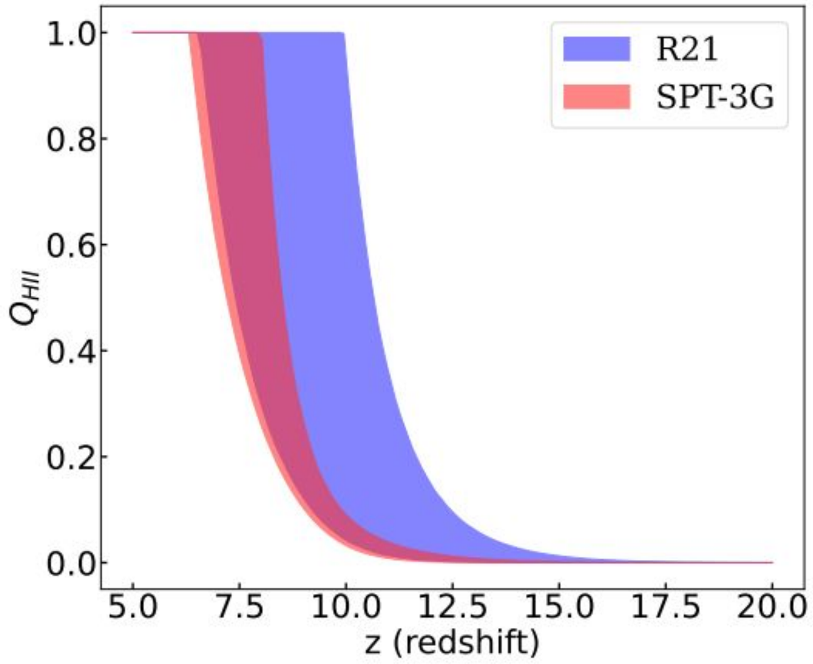

Jain et al. (submitted)
arXiv:2311.00315

Reionization forecast for upcoming experiments

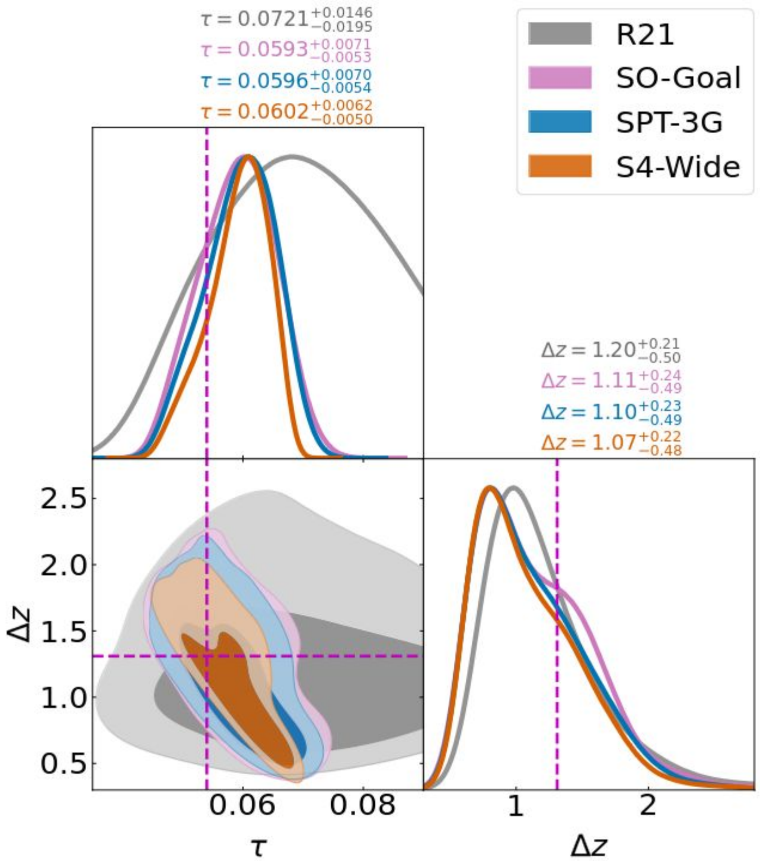

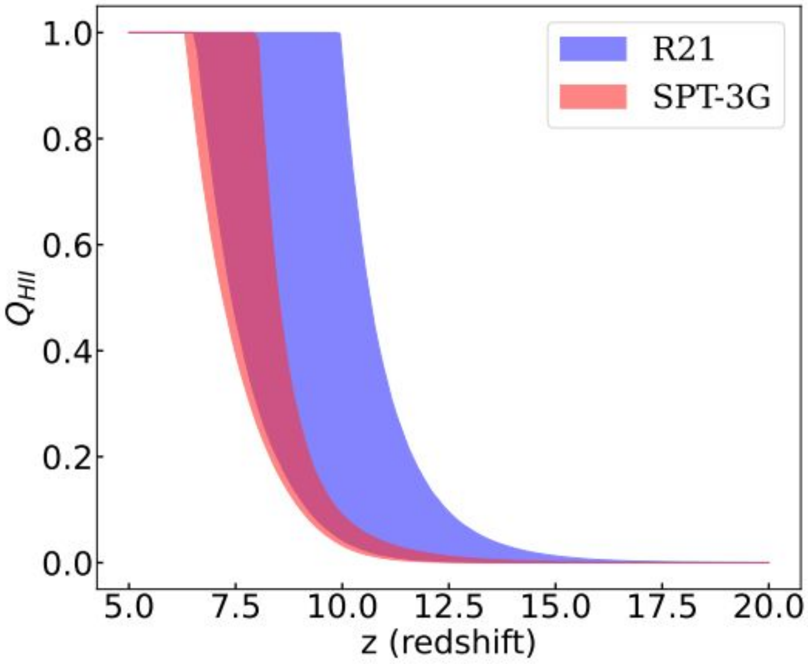

Jain et al. (submitted)
arXiv:2311.00315

Reionization forecast for upcoming experiments

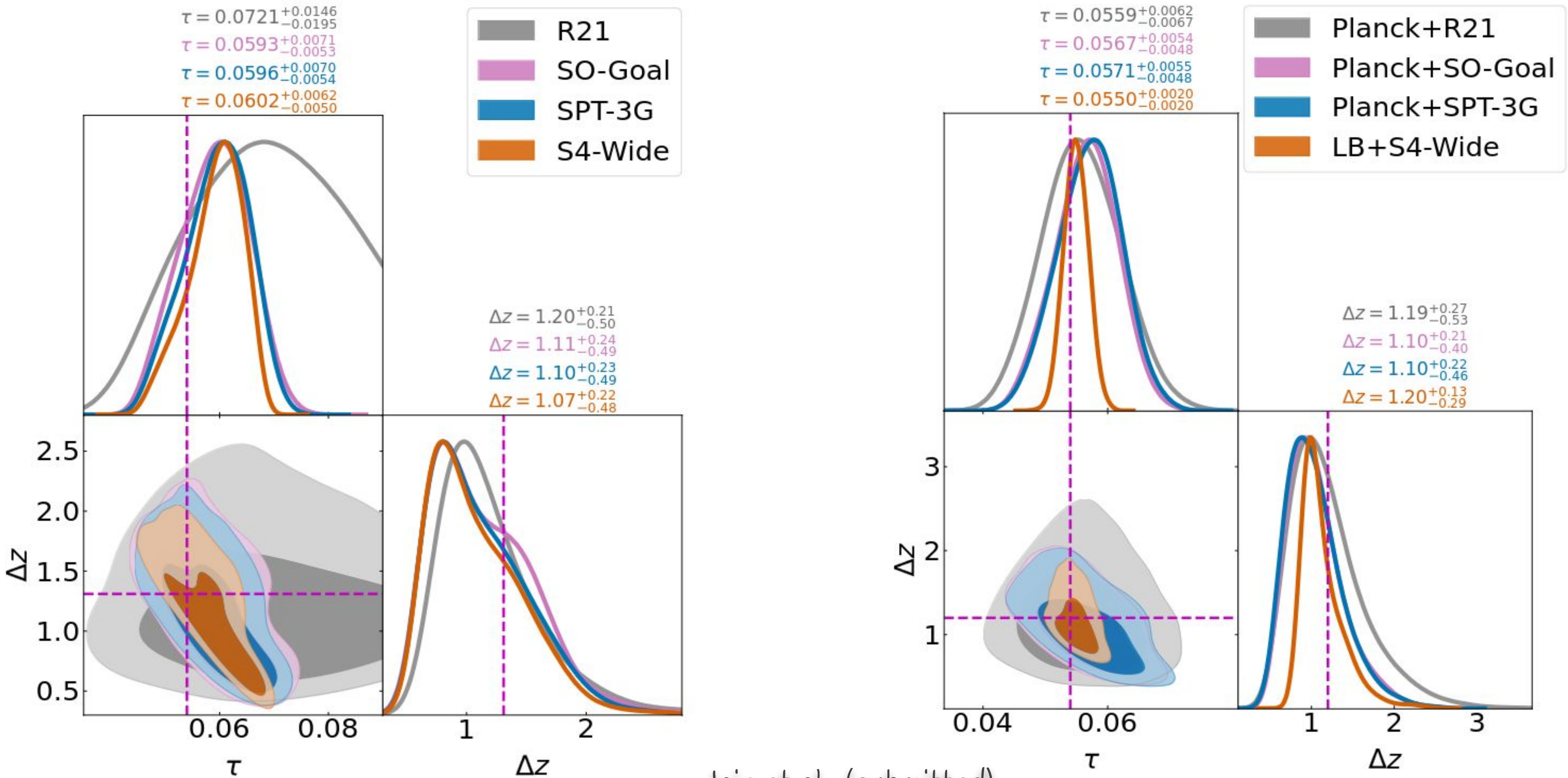

Jain et al. (submitted)
arXiv:2311.00315

Reionization forecast for upcoming experiments

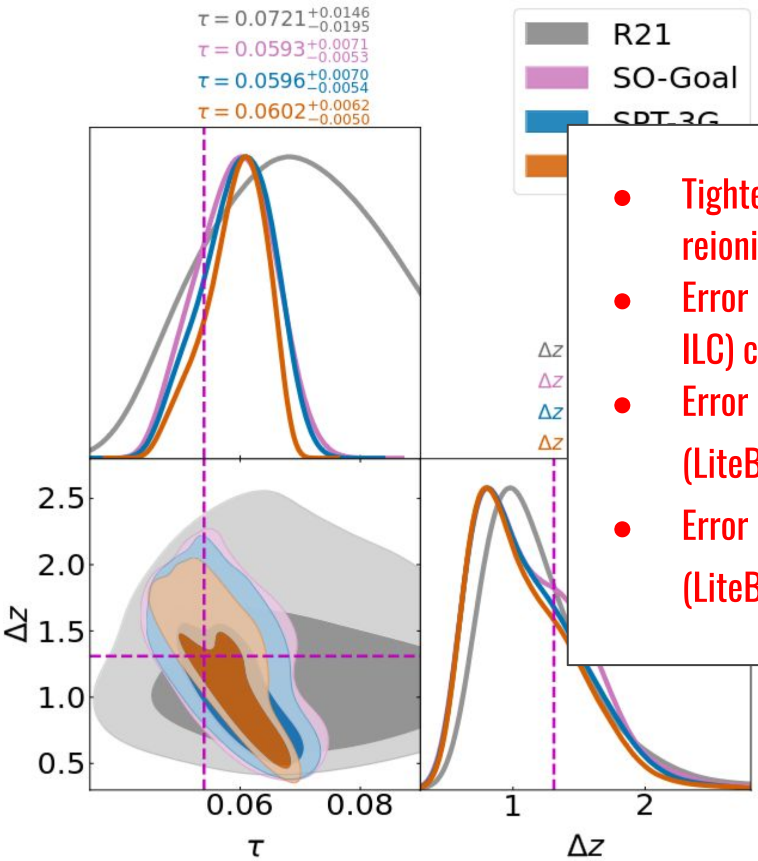

- Tighter constraint on source properties of reionization
- Error bars on $\tau \sim 0.0062$ (SPT-3G Cross ILC) compared to ~ 0.017 (R21)
- Error bars on $z_{50} \sim 0.25$ (LiteBIRD τ + S4-Wide Cross ILC)
- Error bars on $\Delta z \sim 0.21$ (LiteBIRD τ + S4-Wide Cross ILC)

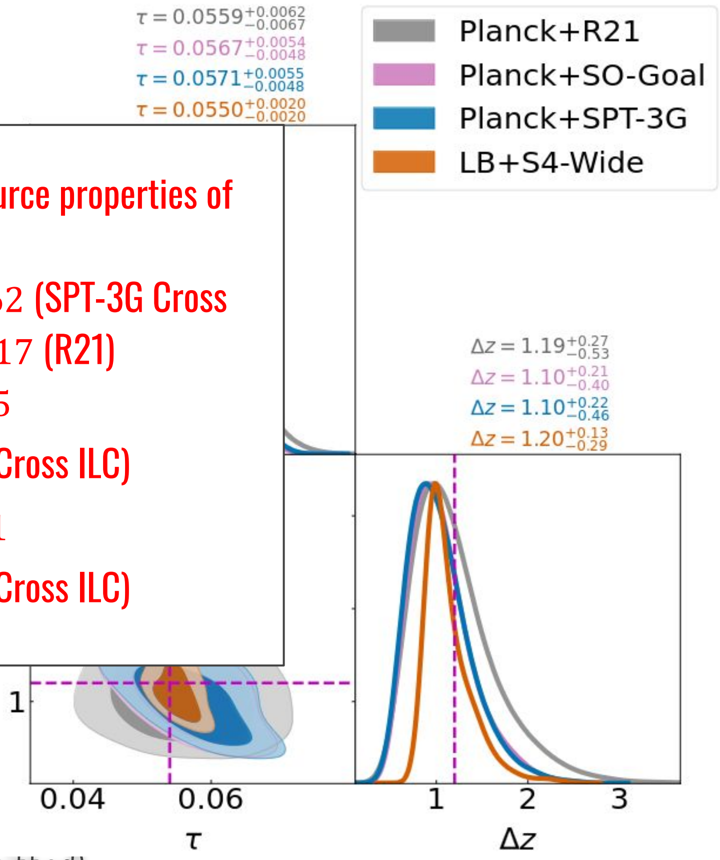

Jain et al. (submitted)
arXiv:2311.00315

What next? Beyond the power spectrum!

- kSZ is an integrated signal!
- Cross- Correlating with redshift based probes (e.g. 21-cm power spectrum) will enable decomposing of the kSZ's line of sight integral.

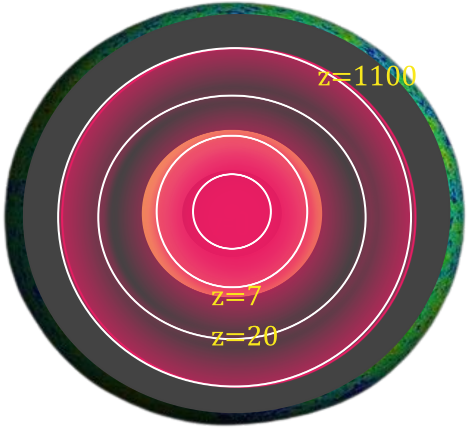

What next? Beyond the power spectrum!

- kSZ is an integrated signal!
- Cross- Correlating with redshift based probes (e.g. 21-cm power spectrum) will enable decomposing of the kSZ's line of sight integral.
- With SCRIPT we have now created the most consistent kSZ maps.
- This will enable the possibility of studying the ionization topology as well as large-scale properties at reionization redshifts.
  [To be done!]

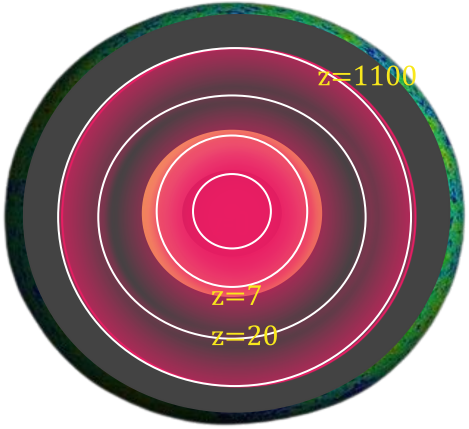

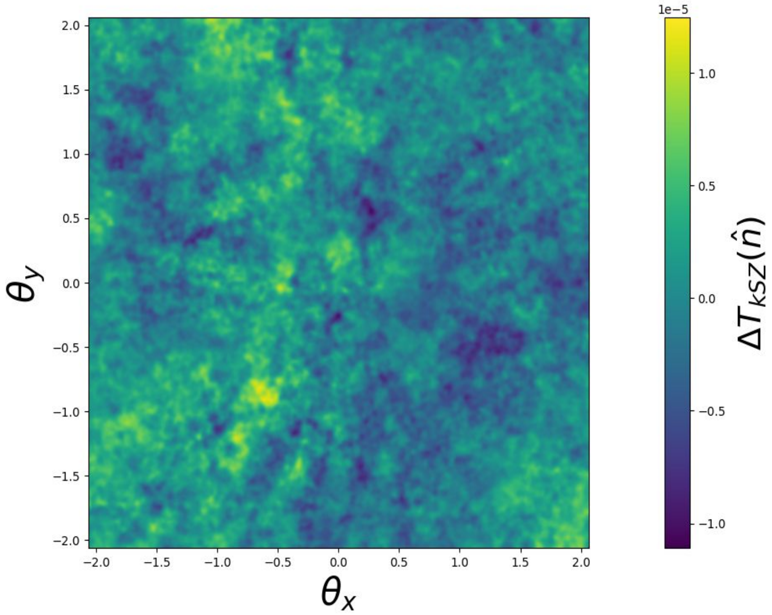

Summary:

1. CMB provides a complimentary picture to 21 cm observations from reionization era.
2. CMB Thomson scattering optical depth provides access to evolution of mean ionized fraction while kSZ will help constraint the patchiness in the reionization era.
3. We have developed a self-consistent framework to evaluate the CMB anisotropies of reionization.
4. Current constraints:
   a. indicative of suppressed star formation in low mass haloes as a result of radiative feedback
   b. indicative of more efficient cooling and star formation or increased escape fraction at lower redshifts.
   c. Duration of reionization constrained at $\Delta z = 1.19^{+0.27}_{-0.53}$
5. Cross-ILC technique will enable access to the shape of power spectrum
   a. Unprecedented constraints on patchiness of reionization
   b. Error bars on $z_{50} \sim 0.25$ (LiteBIRD τ + S4-Wide Cross ILC)
   c. Error bars on $\Delta z \sim 0.21$ (LiteBIRD τ + S4-Wide Cross ILC)
6. To do list:
   a. Use the 21 cm observations to decompose the integrated information in CMB observations
   b. Going beyond 2-point statistics with maps

Patchy Reionization Bias On Tensor-to-Scalar ratio r

1. Gravitational Waves (GWs) are prediction of Inflationary models *(Kamionkowski 2016)*
2. GWs produce B mode polarization.
3. The amplitude of B-mode is tied to the tensor-to-scalar power spectrum ratio r.
4. The latest constraint on r :
   a. $r < 0.035$ (95% C.L.) *(BICEP3 2022)*

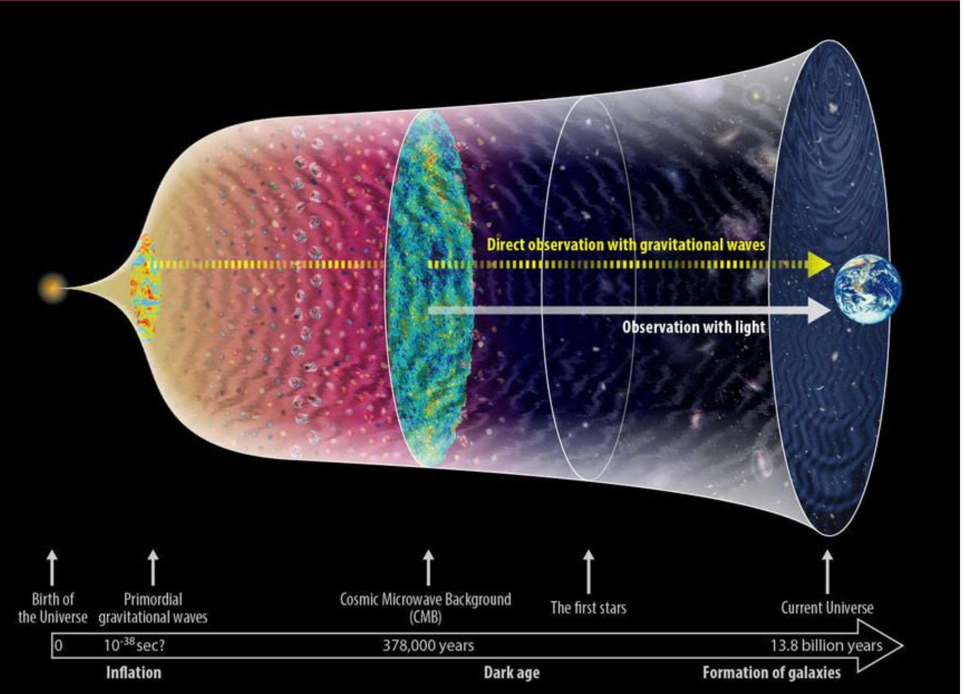

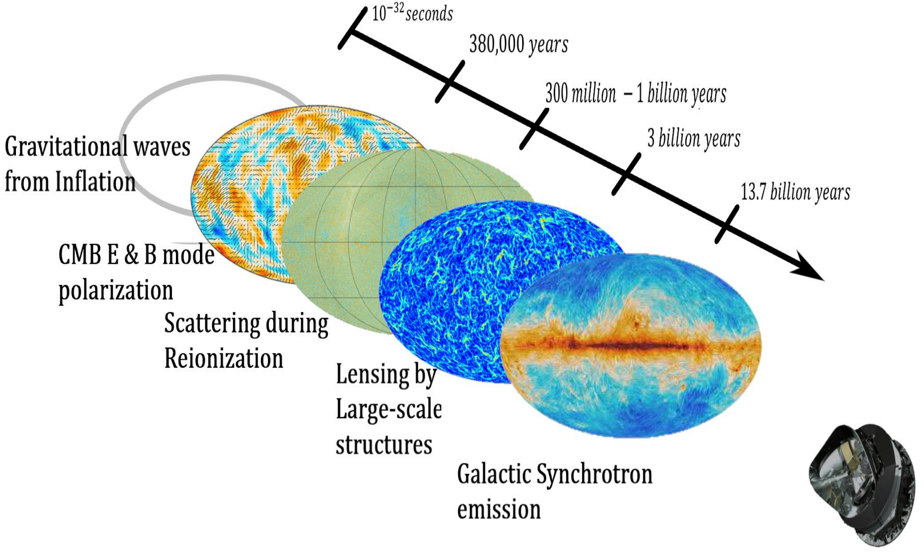

Framework to forecast bias on r

Jain et al. 2023

Likelihood function:

$$-2\log\mathcal{L} = \left(\frac{\tau-\tau^{\rm obs}}{\sigma_\tau^{obs}}\right)^2 + \left(\frac{D^{\rm kSZ}_{\ell=3000}-D^{\rm kSZ,obs}_{\ell=3000}}{\sigma^{\rm kSZ,obs}_{\ell=3000}}\right)^2 + \sum_{\ell=\ell_{min}}^{\ell_{max}}\left(\frac{D_\ell^{BB}-D_\ell^{BB,obs}}{\Sigma_\ell}\right)^2$$

$$\text{Template}:\ D_\ell^{BB} = D_\ell^{BB,\rm prim} + A_{\rm lens}D_\ell^{BB,\rm lens} + D_\ell^{BB,\rm reion}$$

$$\text{Template}-D_\ell^{BB,\rm reion}:\ D_\ell^{BB} = D_\ell^{BB,\rm prim} + A_{\rm lens}D_\ell^{BB,\rm lens}$$

To study bias, the idea is the following :

- Inference of r for the model $\text{Template}-D_\ell^{BB,\rm reion}$ corresponds to a biased recovery of r.
- Post inference of r for each model, bias is:

$$\frac{\Delta r}{\sigma} \equiv \frac{\left(r_{\rm Template} - r_{{\rm Template}-D_\ell^{BB,\rm reion}}\right)}{\sigma_{r_{\rm Template}}}$$

Template — — Template $- D_\ell^{BB,\rm reion}$

Pessimistic case of bias with CMB-S4

mock r =1e-3
85% delensing
Best-fit reionization model

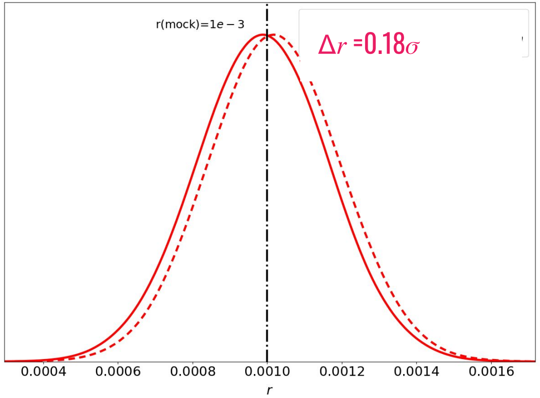

Optimistic case of bias with PICO:

mock r =5e-4
95% delensing
extreme reionization model

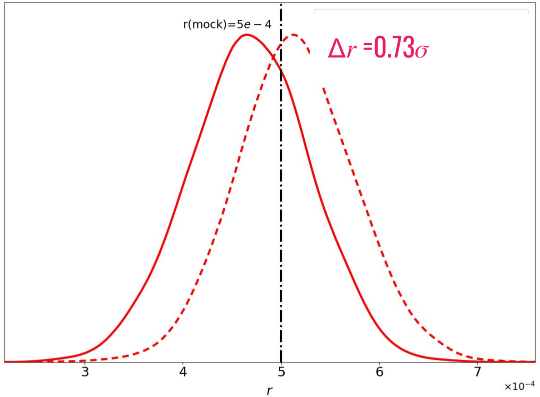

Framework to forecast bias on r

Jain et al. 2023

Template   Template $- D_\ell^{BB,\mathrm{reion}}$

Likelihood function:

$$-2\log\mathcal{L} = \left(\frac{\tau-\tau^{\mathrm{obs}}}{\sigma_\tau^{obs}}\right)^2 + \left(\frac{D^{\mathrm{kSZ}}_{\ell=3000} - D^{\mathrm{kSZ,obs}}_{\ell=3000}}{\sigma^{\mathrm{kSZ,obs}}_{\ell=3000}}\right.$$

$$\sum_{\ell=\ell_{min}}^{\ell_{max}}\left(\frac{D_\ell^{BB}-D_\ell^{BB,obs}}{\Sigma_\ell}\right)^2$$

$$\mathrm{Template}: \ D_\ell^{BB} = D_\ell^{BB,\mathrm{prim}} + A_{\mathrm{lens}}D_\ell^{BB}$$

$$\mathrm{Template} - D_\ell^{BB,\mathrm{reion}}: \ D_\ell^{BB} = D_\ell^{BB,\mathrm{prim}} +$$

To study bias, the idea is the following :

- Inference of r for the model Templ
  corresponds to a biased recovery of r.
- Post inference of r for each model, bias as:

$$\frac{\Delta r}{\sigma} \equiv \frac{\left(r_{\mathrm{Template}} - r_{\mathrm{Template}-D_\ell^{BB,\mathrm{reion}}}\right)}{\sigma_{r_{\mathrm{Template}}}}$$

Pessimistic case of bias with CMB-S4

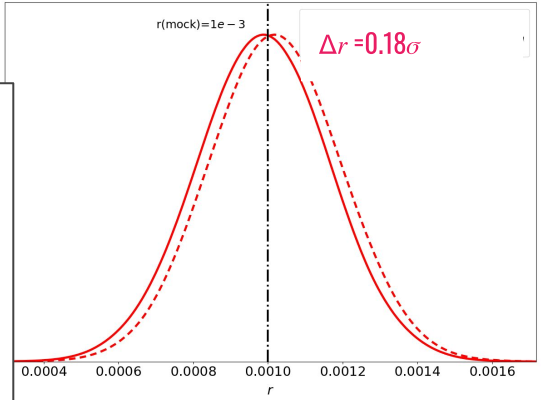

- Inaccurate B-mode power modelling biases r =1e-3 measurement, lowering detection significance from 5σ to ~4.8σ.
- With extreme reionization and efficient delensing, detection claims for r = 5e-4 influenced by a ~0.73σ bias.
- Combining CMB observables we can constrain patchy reionization and mitigate its impact on the value of r.

c case of bias with PICO:

extreme reionization model

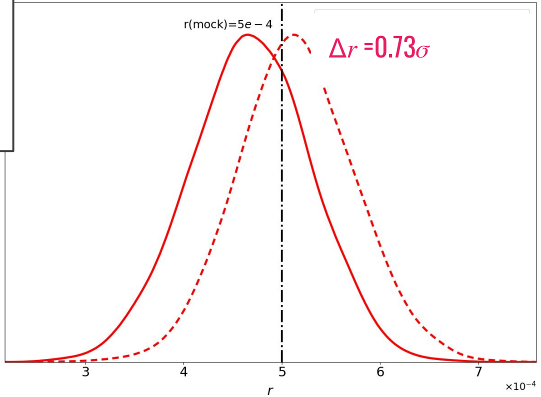

Patchy free electron distribution and τ power spectrum

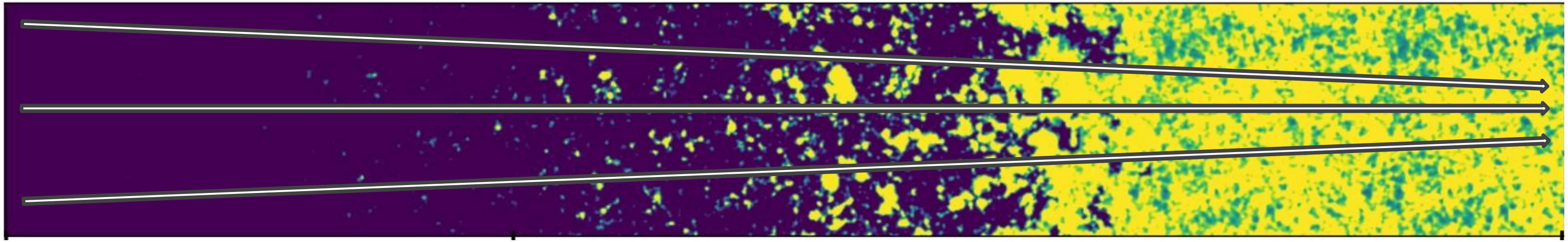

Reionization era free electron evolution

$$x_e\,(\hat{n},\chi) = \bar{x}_e\,(\chi) + \Delta x_e(\hat{n},\chi) \qquad x_e \equiv n_e/n_H$$

Global mean — Fluctuation

$$\tau(\hat{n}) = \bar{\tau} + \Delta\tau(\hat{n}) \Longrightarrow \sum \tau_{\ell,m} Y_{\ell,m} \Longrightarrow <\tau_{\ell,m}\tau^*_{\ell,m}> \Longrightarrow C_\ell^{\tau\tau}$$

Patchy optical depth

τ power spectrum

Captures ionization fluctuation in n_e

$$C_\ell^{\tau\tau} = (\sigma_T \bar{n}_{H,0})^2 \int \frac{d\chi}{a^4\chi^2} P_{ee}\left(k = \frac{\ell}{\chi}, \chi\right)$$

Gaining insights with τ power spectrum

1. Simplistic spherical bubble-based prescriptions become inaccurate when individual ionized bubbles begin to overlap.
2. More realistic numerical methods need to be employed to explore the prospect of constraining patchy reionization using estimates of the patchy τ field.

1. Dvorkin & Smith 2009 and Roy et al. 2018:
   a. Dvorkin & Smith 2009 presented the estimators to extract the τ power from CMB data sets
   b. Explored dependence of tau power spectrum on bubble based reionization configuration.
   c. Detected patchy reionization signal for a characteristic bubble radius of 5 Mpc with $(S/N)>5$ allowed by τ constraints from respective cosmologies , WMAP 2009 & Planck 2016.
2. Meerburg et al. 2013:
   a. Used three-point τ-21 cm correlation statistics to constrain the reionization timeline.
   b. With optimistic experiment sensitivities, Reionization width can be constrained with an error bar of 10%.
   c. Optical depth tau can be constrained with an error bar of 4%.

Detectability of tau power spectrum

Noise power spectrum is evaluated using the EB Minimum Variance Estimator (Dvorkin & Smith 2009)

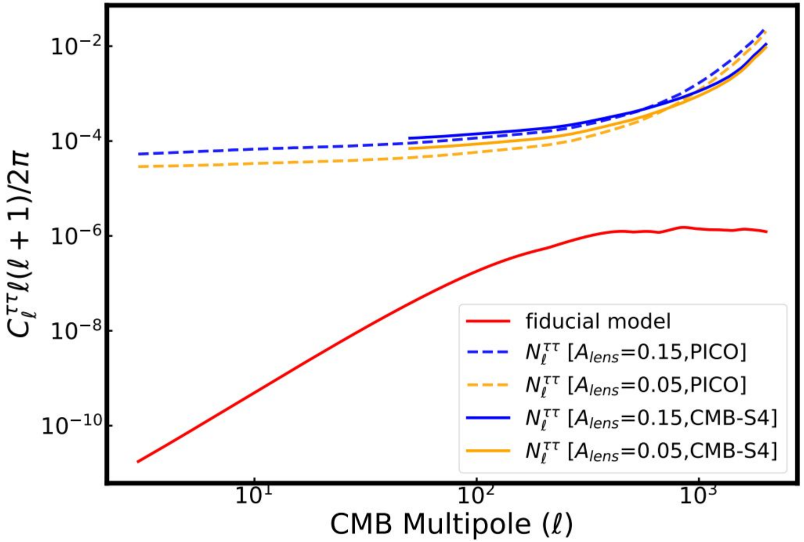

τ-power spectrum and noise power spectrum at different delensing scenarios corresponding to observations with CMB-S4 and PICO.

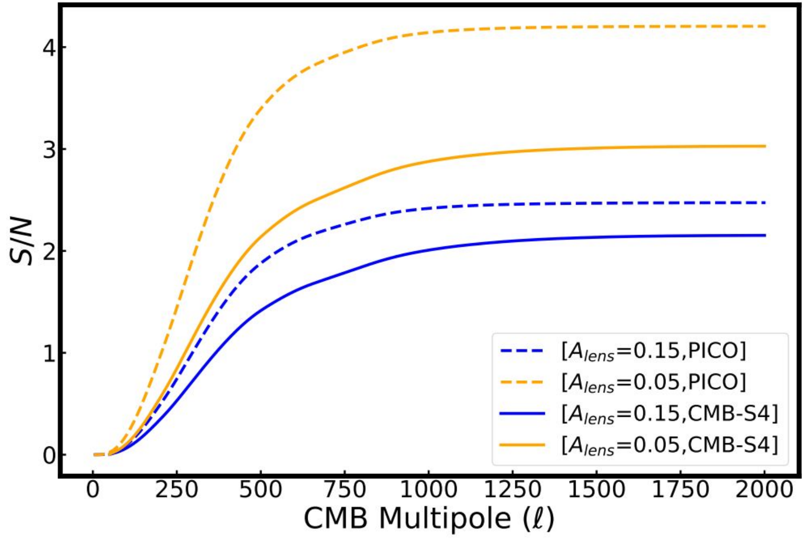

Cumulative signal-to-ratio at different delensing scenarios corresponding to observations with CMB-S4 and PICO.

Takeaway: A $\gtrsim 3\sigma$ detection for the τ-power spectrum is possible for both the instruments at a 95% delensing.

Constraints on physical model of reionization

Inclusion of τ-power spectrum leads to tighter constraints on α_ζ .

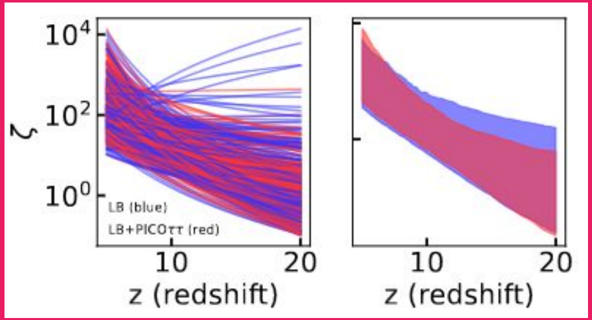

LB (blue)
LB+PICO$\tau\tau$ (red)

1. $D^{BB}_{\ell=200}\,(\mathrm{nK}^2)$ constraints at, with errors improving from 1.89 (LB) to 1.45 (LB+PICO$\tau\tau$)
2. $D^{\tau\tau}_{\ell=400} \times 10^6$ errors decrease from 0.83 (LB) to 0.26 (LB+PICO$\tau\tau$).
3. Δz from error bars of ~ 0.44 (LB) to ~ 0.36 (LB+PICO$\tau\tau$)

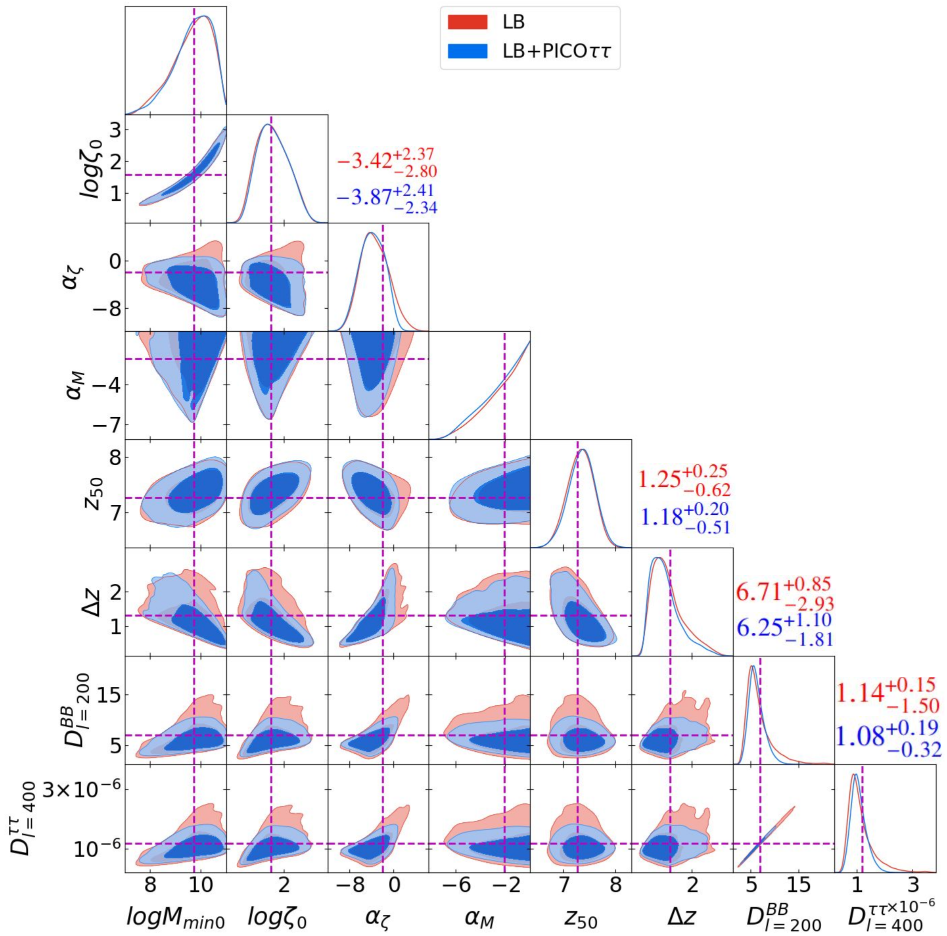

Constraints on physical model of reionization

Inclusion of τ-power spectrum leads to tighter constraints on α_ζ .

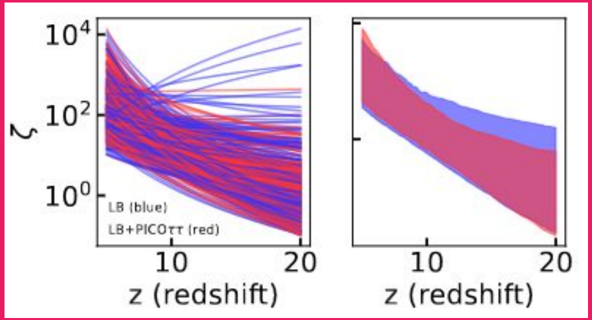

LB (blue)
LB+PICO$\tau\tau$ (red)

1. $D^{BB}_{\ell=200}(\mathrm{nK}^2)$ constraints at, with errors improving from 1.89 (LB) to 1.45 (LB+PICO$\tau\tau$)
2. $D^{\tau\tau}_{\ell=400} \times 10^6$ errors decrease from 0.83 (LB) to 0.26 (LB+PICO$\tau\tau$).
3. Δz from error bars of ~ 0.44 (LB) to ~ 0.36 (LB+PICO$\tau\tau$)

$$C_\ell^{BB,\mathrm{reion}} \approx \frac{3}{100} C_\ell^{\tau\tau} Q^2_{\mathrm{rms}} e^{-2\tau}$$

(Dvorkin et al. 2010)

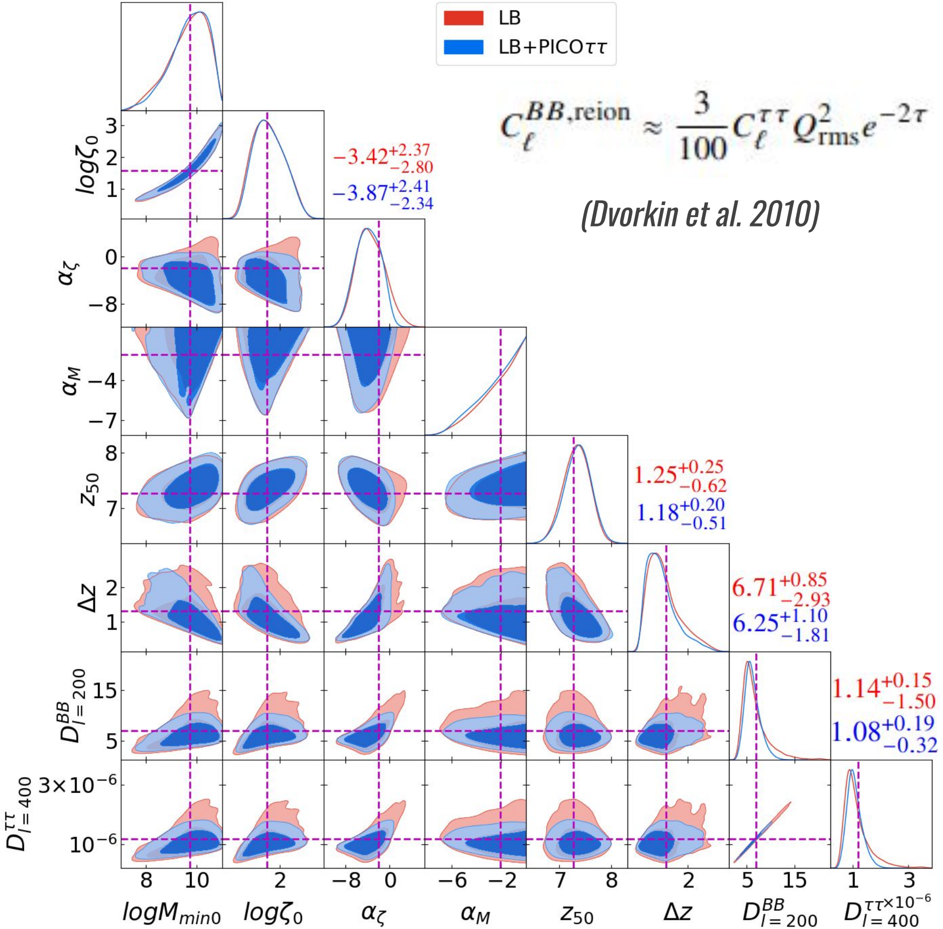

Detectability of Patchy B mode

- Detecting the patchy B-mode signal will be an essential step towards "detau"-ing the primordial B-mode signal, leading to the unbiased measurement of the tensor-to-scalar power spectrum ratio r.
- Shape of the B-mode power spectrum is different for patchy reionization and primordial gravitational waves
- Shape of the patchy-B mode power spectrum remains roughly constant over the range while amplitude is a function of the details of reionization process.

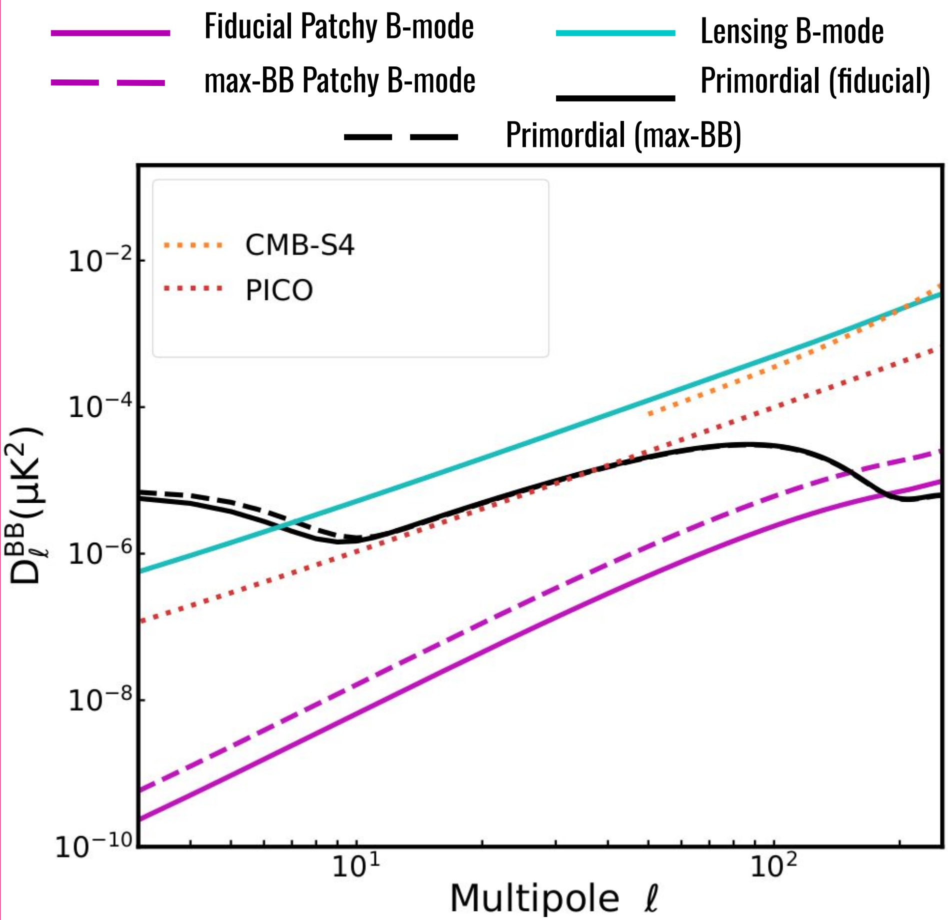

Exploiting synergy : scattering B-mode & τ power spectrum

- Opportunity to detect patchy reionization in nearly model-independent manner with Stage-4 CMB experiments by exploiting the synergy between τ and B-mode power spectrum
- Infer the signal of both primordial gravitational waves and patchy reionization jointly from the CMB data.

Model B-mode signal: Measures patchiness in the reionization B-mode

$$C_\ell^{BB} = C_\ell^{BB,prim} + A_{lens} C_\ell^{BB,lens} + \boxed{A_\tau} C_{\ell,\mathrm{fid}}^{BB,\mathrm{reion}}$$

Constraining A_τ with projected τ and B-mode data:

$$-2\log\mathcal{L} = \left(\frac{\tau - \tau^{\mathrm{obs}}}{\sigma_\tau^{obs}}\right)^2 + \sum_\ell \left(\frac{\bar{C}_\ell^{BB} - C_\ell^{BB}}{\Sigma_\ell^{BB}}\right)^2.$$

Analytical relation between patchy-B mode and the τ-power spectrum: *(Dvorkin et al. 2010)*

$$\boxed{C_\ell^{BB,\mathrm{reion}}} \approx \frac{3}{100} \boxed{C_\ell^{\tau\tau}} Q_{\mathrm{rms}}^2 e^{-2\tau}$$

Constraining A_τ with projected polarization data:

$$-2\log\mathcal{L} = \left(\frac{\tau - \tau^{\mathrm{obs}}}{\sigma_\tau^{obs}}\right)^2 + \sum_\ell \left(\frac{\bar{C}_\ell^{BB} - C_\ell^{BB}}{\Sigma_\ell^{BB}}\right)^2 + \boxed{\sum_\ell \left(\frac{\bar{C}_\ell^{\tau\tau} - C_\ell^{\tau\tau}}{\Sigma_\ell^{\tau\tau}}\right)^2}$$

Detecting Patchy B-mode:

exploiting synergy with τ-power spectrum

$$C_\ell^{\tau\tau} = (\sigma_T \bar{n}_{H,0})^2 \int \frac{d\chi}{a^4\chi^2} P_{ee}\left(k = \frac{\ell}{\chi}, \chi\right)$$

- Stage-4 CMB experiments will allow near model-independent detection of patchy reionization, exploiting the τ and B-mode power spectrum synergy.
- Infer the signal of both primordial gravitational waves and patchy reionization jointly from the CMB data.

Cumulative signal-to-ratio to detect patchy-τ power at different delensing scenarios corresponding to observations with CMB-S4 and PICO.

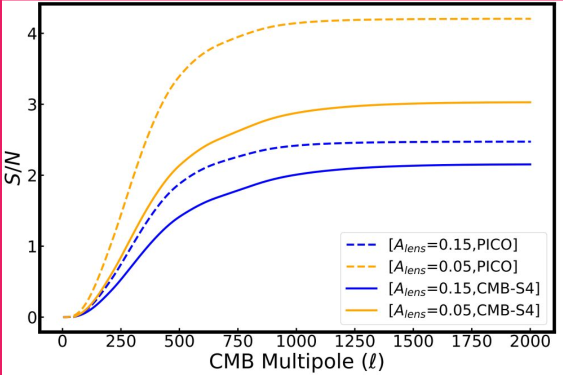

Jain et al. (in prep)

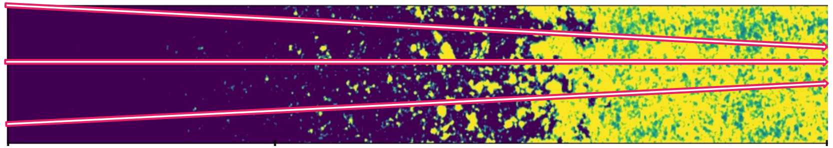

Model B-mode signal:

Measures patchiness in the reionization era

$$C_\ell^{BB} = C_\ell^{BB,prim} + A_{lens} C_\ell^{BB,lens} + A_\tau C_{\ell,\mathrm{fid}}^{BB,\mathrm{reion}}$$

Constraining A_τ with projected τ and B-mode data:

$$-2\log\mathcal{L} = \left(\frac{\tau - \tau^{\mathrm{obs}}}{\sigma_\tau^{obs}}\right)^2 + \sum_\ell \left(\frac{\bar{C}_\ell^{BB} - C_\ell^{BB}}{\Sigma_\ell^{BB}}\right)^2.$$

Analytical relation between patchy-B mode and the τ-power spectrum: *(Dvorkin et al. 2010)*

$$C_\ell^{BB,\mathrm{reion}} \approx \frac{3}{100} C_\ell^{\tau\tau} Q_{\mathrm{rms}}^2 e^{-2\tau}$$

Constraining A_τ with projected polarization data:

$$-2\log\mathcal{L} = \left(\frac{\tau - \tau^{\mathrm{obs}}}{\sigma_\tau^{obs}}\right)^2 + \sum_\ell \left(\frac{\bar{C}_\ell^{BB} - C_\ell^{BB}}{\Sigma_\ell^{BB}}\right)^2 + \sum_\ell \left(\frac{\bar{C}_\ell^{\tau\tau} - C_\ell^{\tau\tau}}{\Sigma_\ell^{\tau\tau}}\right)^2$$

Forecasts on A_τ with Stage-4 CMB experiments

Jain et al. (in prep)

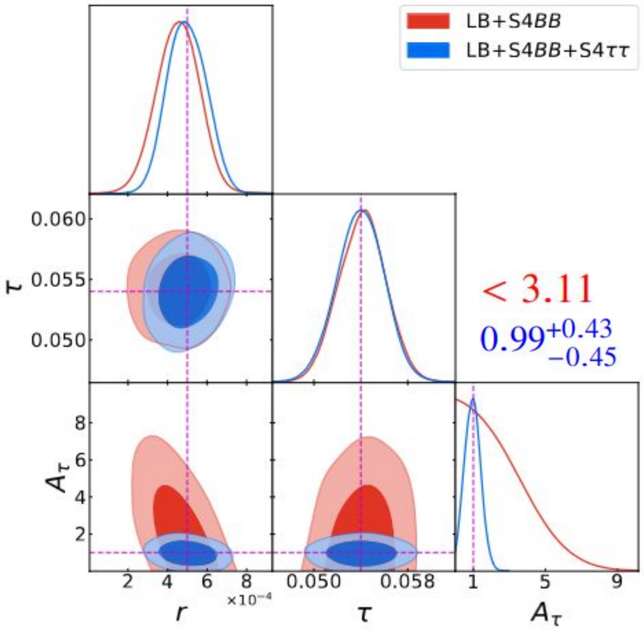

LB+CMB-S4 data sets: A_τ/σ_{A_τ} = 2.25

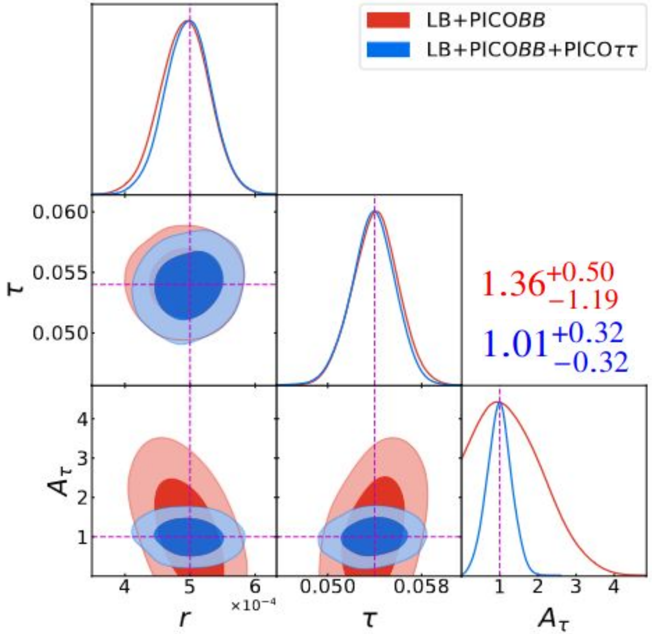

LB+PICO data sets: A_τ/σ_{A_τ} = 3.16

Forecasts on A_τ with Stage-4 CMB experiments

Jain et al. (in prep)

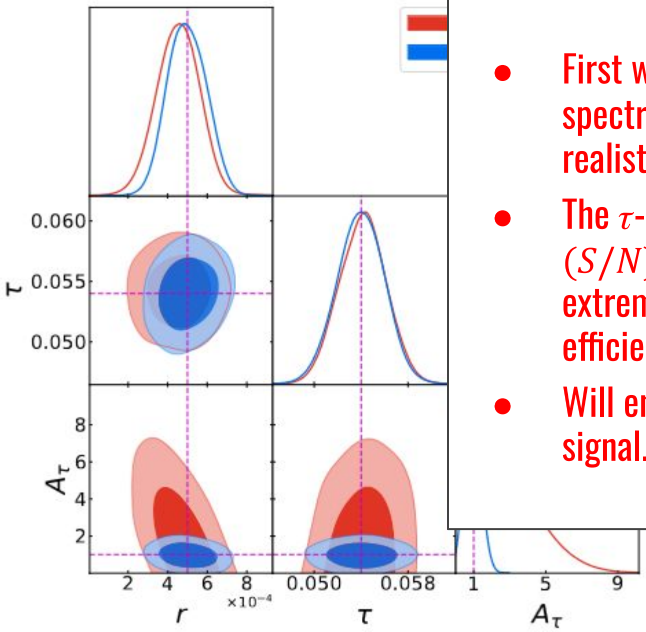

LB+CMB-S4 data sets: A_τ/σ_{A_τ} = 2.25

- First work to assess the patchy τ-power spectrum's detectability using physical, realistic reionization models.
- The τ-power spectrum is detectable at $(S/N) \sim 3$, improving to $(S/N) \geq 6$ in extreme reionization scenarios, given efficient delensing.
- Will enable detection of the patchy B-mode signal.

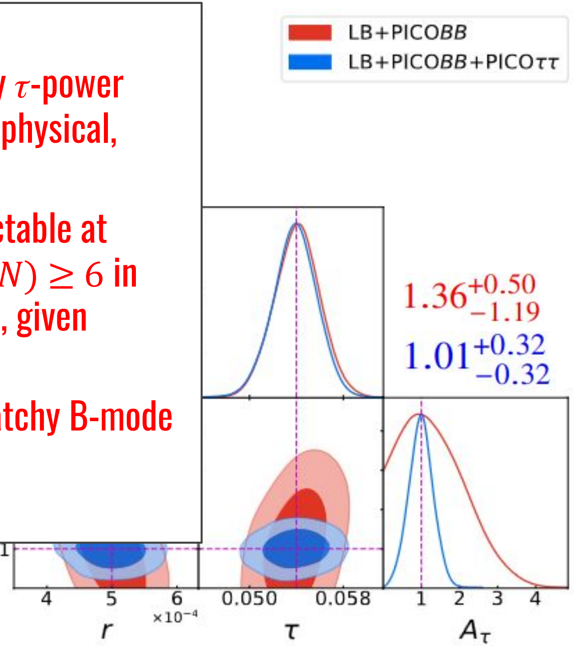

LB+PICO data sets: A_τ/σ_{A_τ} = 3.16

Modelling reionization imprints on CMB 101:

Principal Ingredient : Ionized Hydrogen field

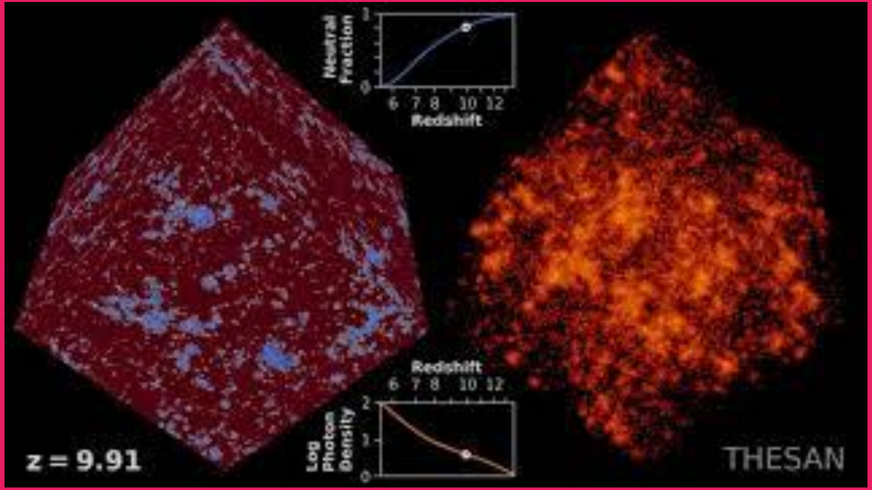

Volume rendering of the HI fraction (left) and ionizing radiation field (right) in the Thesan-1 simulation

Building blocks of reionization:

- Cosmology and structure formation
- Galaxy formation and the interstellar medium
- Radiation propagation through the intergalactic medium

Classification of reionization models based on complexity:

- Full numerical models
- Analytical and semi-analytical models
- Semi-numerical models

Advantages of semi-numerical schemes:

- A compromise between full numerical and analytical models.
- Can capture some non-linearities that analytical models cannot.
- Computationally expensive but more feasible than full simulations.